Quarterly Technical Report

Growth, Characterization and Device Development in Monocrystalline Diamond Films

Supported under Grant #N00014-93-I-0437
Office of the Chief of Naval Research
Report for the period 10/1/97–12/31/97

R. F. Davis, R. J. Nemanich* and Z. Sitar
P. K. Baumann*, W. Liu, R. Schlesser, A. T. Sowers*,
B. L. Ward*, C. A. Wolden, and P. C. Yang
North Carolina State University
c/o Materials Science and Engineering Department
*Department of Physics
Box 7907
Raleigh, NC 27695

December, 1997

REPORT DOCUMENTATION PAGE

Form Approved
OMB No. 0704-0188

1. AGENCY USE ONLY *(Leave blank)*	2. REPORT DATE	3. REPORT TYPE AND DATES COVERED
	December, 1997	Quarterly Technical 10/1/97-12/31/97

4. TITLE AND SUBTITLE

Growth, Characterization and Device Development in Monocrystalline Diamond Films

5. FUNDING NUMBERS

s400003srr14
1114SS
N00179
N66005
4B855

6. AUTHOR(S)

R. F. Davis, R. J. Nemanich, and Z. Sitar

7. PERFORMING ORGANIZATION NAME(S) AND ADDRESS(ES)

North Carolina State University
Hillsborough Street
Raleigh, NC 27695

8. PERFORMING ORGANIZATION REPORT NUMBER

N00014-93-I-0437

9. SPONSORING/MONITORING AGENCY NAMES(S) AND ADDRESS(ES)

Sponsoring: ONR, Code 312, 800 N. Quincy, Arlington, VA 22217-5660
Monitoring: Admin. Contracting Officer, Office of Naval Research
Atlanta Regional Office
100 Alabama Street, Suite 4R15
Atlanta, GA 30303

10. SPONSORING/MONITORING AGENCY REPORT NUMBER

11. SUPPLEMENTARY NOTES

12a. DISTRIBUTION/AVAILABILITY STATEMENT

Approved for Public Release; Distribution Unlimited

12b. DISTRIBUTION CODE

13. ABSTRACT ***(Maximum 200 words)***

The growth of coalesced, highly-oriented diamond films has been achieved on nickel substrates using a multi-step process consisting of (1) seeding the Ni surface with 0.5 μm diamond powder, (2) annealing at 1100°C in a hydrogen atmosphere, and (3) growth at 900°C in a mixture of hydrogen and 0.5% methane. An addition of 0.5% methane in the gas phase produced optimum results, as the nucleation density, orientation of diamond particles, and uniformity were substantially improved. Substrates nucleated under these conditions were grown out into coalesced, 30 μm thick films. Both (100) and (111) oriented films showed a high degree of orientation and Raman spectra obtained from these orientations showed intense and narrow diamond signature peaks with FWHMs of 5 and 8 cm^{-1}, respectively. Nitrogen-doped diamond was deposited by microwave plasma CVD for cold cathode applications and characterized by laser reflectance interferometry, Raman and photoluminescence spectroscopies, and field emission measurements. Initially growth rates of diamond films were enhanced by nitrogen addition, but further nitrogen addition caused a decrease in the growth rate and eventually no diamond deposition was observed for [N]/[C] gas phase ratios greater than 70. Raman scattering spectroscopy indicated a decrease in film quality with nitrogen doping. Field emission measurements indicate threshold fields of 70-90 V/mm independent of process conditions. It was also observed that hydrogen leads to a negative electron affinity (NEA) on diamond(100) surfaces while oxygen termination and adsorbate-free surfaces exhibit a positive electron affinity. Zirconium deposited on clean and oxygen- or hydrogen-containing diamond(100) surfaces also exhibited an NEA.

14. SUBJECT TERMS

diamond, thin film, nickel substrates , Raman, nitrogen, microwave plasma CVD, cold cathode, laser reflectance interferometry, photoluminescence, field emission, growth rates, negative electron affinity, oxygen termination, hydrogen, zirconium

15. NUMBER OF PAGES

67

16. PRICE CODE

17. SECURITY CLASSIFICATION OF REPORT	18. SECURITY CLASSIFICATION OF THIS PAGE	19. SECURITY CLASSIFICATION OF ABSTRACT	20. LIMITATION OF ABSTRACT
UNCLAS	UNCLAS	UNCLAS	SAR

Table of Contents

I. Introduction

Diamond as a semiconductor in high-frequency, high-power transistors has unique advantages and disadvantages. Two advantages of diamond over other semiconductors used for these devices are its high thermal conductivity and high electric-field breakdown. The high thermal conductivity allows for higher power dissipation over similar devices made in Si or GaAs, and the higher electric field breakdown makes possible the production of substantially higher power, higher frequency devices than can be made with other commonly-used semiconductors.

In general, the use of bulk crystals severely limits the potential semiconductor applications of diamond. Among several problems typical for this approach are the difficulty of doping the bulk crystals, device integration problems, high cost and low area of such substrates. In principal, these problems can be alleviated via the availability of chemically vapor deposited (CVD) diamond films. Recent studies have shown that CVD diamond films have thermally activated conductivity with activation energies similar to crystalline diamonds with comparable doping levels. Acceptor doping via the gas phase is also possible during activated CVD growth by the addition of diborane to the primary gas stream.

The recently developed activated CVD methods have made feasible the growth of polycrystalline diamond thin films on many non-diamond substrates and the growth of single crystal thin films on diamond substrates. More specifically, single crystal epitaxial films have been grown on the {100} faces of natural and high pressure/high temperature synthetic crystals. Crystallographic perfection of these homoepitaxial films is comparable to that of natural diamond crystals. However, routes to the achievement of rapid nucleation on foreign substrates and heteroepitaxy on one or more of these substrates has proven more difficult to achieve. This area of study has been a principal focus of the research of this contract.

At present, the feasibility of diamond electronics has been demonstrated with several simple experimental devices, while the development of a true diamond-based semiconductor materials technology has several barriers which a host of investigators are struggling to surmount. It is in this latter regime of investigation that the research described in this report has and continues to address.

In this reporting period, (1) growth of coalesced, highly-oriented diamond films has been achieved on nickel substrates using a multi-step process, (2) deposition of N-doped diamond films and (3) photoemission and field emission from adsorbate-free and H- and O-terminated diamond surfaces have been achieved. The following sections are self-contained in that they present an introduction, experimental procedures, results and discussion, summary and indications of future research for the given research thrust.

II. Coalesced Oriented Diamond Films on Nickel

P. C. Yang, C. A. Wolden, W. Liu, R. Schlesser, R. F. Davis, J. T. Prater*, and Z. Sitar
Department of Materials Science and Engineering, NCSU, Raleigh, NC 27695-7919
* Army Research Office, RTP, NC 27709

Abstract

The growth of coalesced, highly oriented diamond films has been achieved on nickel substrates using a multi-step process that consisted of (1) seeding the Ni surface with 0.5 μm diamond powder, (2) annealing at 1100°C in a hydrogen atmosphere, and (3) growth at 900°C in a mixture of hydrogen and 0.5% methane. Auger depth profile analysis of a sample quenched after the annealing stage showed presence of significant amounts of carbon (6 at%) close to the substrate surface and about 3 at% deeper in the substrate. The loss of carbon into the substrate resulted in relatively low nucleation density. The addition of methane into the gas phase during the annealing stage proved very effective in compensating for the diffusion. An addition of 0.5% methane in the gas phase produced optimum results, as the nucleation density, orientation of diamond particles, and uniformity were substantially improved. Substrates nucleated under these conditions were grown out into coalesced, 30 μm thick films. Both (100) and (111) oriented films showed a high degree of orientation and Raman spectra obtained from these orientations showed intense and narrow diamond signature peaks with FWHMs of 5 and 8 cm^{-1}, respectively.

Submitted to Journal of Materials Research

Nucleation and growth of coalesced, oriented diamond films on non-diamond substrates is important for many applications. Transition metals, and nickel in particular, are attractive substrates for the heteroepitaxial growth of single crystalline diamond films because of their close lattice match to diamond and their catalytic properties [1]. Dewan and coworkers [2] reported on precipitation of diamond particles from different mixtures of diamond and metal powders. Tachibana *et al.* [3] achieved near heteroepitaxial growth of diamond on (111) platinum. We have observed that under certain conditions and in the presence of atomic hydrogen oriented diamond nuclei form from a supersaturated Ni-C-H surface solution [4].]Following this initial success, we developed a multi-step growth process and achieved reproducible heteroepitaxial nucleation of diamond on Ni substrates [5]. Despite producing oriented and well faceted diamond nuclei on Ni, the nucleation density was rather low and nonuniform across the substrate. This limitation has prevented the production of continuous, oriented diamond films. In this letter, we report on the improvement of the nucleation density and uniformity through methane enrichment during the annealing stage of the process. These advances allowed the first production of coalesced, oriented diamond films on nickel substrates.

Originally, the multi-step process started with diamond powder seeding and high temperature annealing in the presence of atomic hydrogen. Relatively uniform seeding was achieved by applying a 0.5 μm powder suspended in acetone over the nickel substrate. After the acetone had evaporated, the samples were placed into atomic hydrogen environment produced by a hot filament, and rapidly heated to ~1100°C. At this temperature, the seeds rapidly reacted with the Ni substrate and disappeared. As a result a reflective substrate surface was observed. This reflective surface state was crucial for the success of the process, since it indicated a complete reaction between the diamond seeds and the Ni substrate [5]. After this annealing step, the substrate temperature was lowered to ~900°C and diamond films were grown for prolonged times in a hydrogen atmosphere containing 0.5% of methane.

The observed rapid disappearance of the diamond seeds (less than 30 s after reaching the high temperature) could be accounted for by two possible mechanisms: (1) dissolution and diffusion of carbon into the nickel substrate, or (2) by etching off the seeds by atomic hydrogen. The latter possibility was discounted by an experiment where a Si wafer was used as a substrate and processed under conditions identical to those used for nickel. In this case the diamond seeds remained almost intact even after prolonged processing times. Therefore, the seeds must have been dissolved in the nickel substrate.

To gain information on the amount of carbon present in the nickel substrate, Auger depth profile analysis was conducted on a sample that was quenched immediately following the high temperature anneal, and prior to the growth step. The quenched sample was polished under a small angle (0.85°) with respect to the surface, for the purpose of determining the depth profile

of carbon species by an Auger line scan. Figure 1a shows a schematic of the prepared sample. The scan from A to B measured the surface of the sample, while the scan from B to D examined the subsurface species. The obtained carbon profile (Figure 1b) shows three distinct regions across the sample: (1) the surface (A to B) is characterized by a constant, high concentration of carbon, (2) the carbon concentration then falls off in a short transition region (B to C) before (3) leveling out at a constant value deeper in the bulk of the substrate(C to D). Auger depth profile measurements performed on a larger scale showed that region (3) extended more than 20 μm into the sample. It is important to note that the virgin substrates did not contain a detectable amount of carbon. This indicated that carbon diffusion under the annealing conditions was very rapid. Using the atomic sensitivity factors, the surface carbon

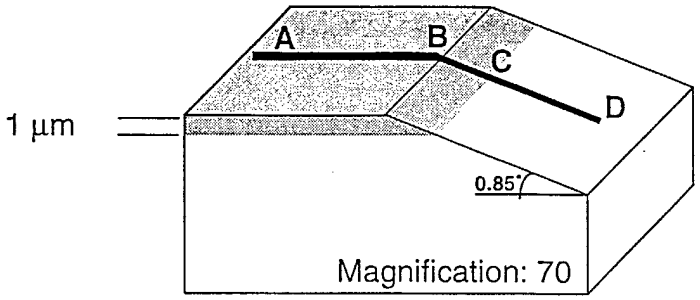

(a)

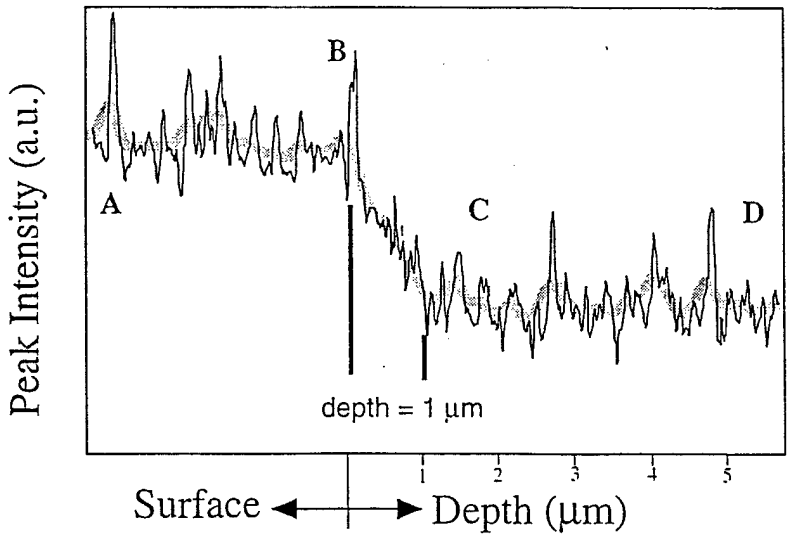

(b)

Figure 1. (a) Schematic of the wedge polished Ni substrate and (b) result of the line scan Auger analysis.

concentration was estimated to be about 6 atomic % and the level in the bulk was about 3 atomic %. The measured carbon content of 3 atomic % corresponds well to the known solubility limit of carbon in nickel [6]. The higher carbon content at the surface may be explained by the conjecture of a molten surface eutectic layer in which a larger amount of carbon was dissolved. From the angle of the wedge, the thickness of the transition region was calculated to be on the order of 1 μm.

As shown by the Auger results, a significant fraction of carbon species diffused into the bulk of the Ni substrate and thus did not contribute to the nucleation process at the surface. In order to counter the loss of carbon into the substrate and maintain a supersaturated surface region, gas-phase enrichment was attempted by introducing the methane during the high temperature annealing step. During the enrichment studies, the methane concentration in the gas phase was varied between 0.5 and 2.5%. Following the annealing, the films were grown at standard conditions (0.5% methane in hydrogen) for short times (5-15 minutes) to evaluate the nucleation density. Samples were examined by scanning electron microscopy (SEM). They all showed a nucleation density on the order of $10^8/cm^2$, which was almost one order of magnitude higher than without the enrichment. Although the initial crystallites were clearly oriented, accurate orientational measurements would have required extreme magnification. Thus, for the purpose of orientational studies, samples were grown for 6 hours after an anneal at different levels of methane enrichment.

Figures 2(a-c) show SEM micrographs of samples obtained with 0.5, 1, and 2.5% of methane enrichment during the annealing step. A perusal of Figure 2a showed that approximately 90% of the crystallites were oriented. The crystallite density was now about $3\times10^6/cm^2$, showing that significant coalescence had already occurred. With 1.0% CH_4 enrichment (Figure 2b), the fraction of oriented particles decreased to about 80%, at a similar crystallite density (5×10^6 /cm^2). Increasing the methane further to 2.5% CH_4 (Figure 2c) decreased the fraction of oriented particles to 50%, while the density remained practically unchanged. By comparing the results obtained at different pretreatment conditions, it was determined that 0.5% of methane in hydrogen gave the highest degree of oriented diamond while also increasing the nucleation density.

While the degree of orientation with 0.5% CH_4 enrichment was similar to previous results obtained with hydrogen only during the high temperature annealing process, both the density and uniformity of the oriented diamond crystallites produced by the new process were significantly improved. The methane addition during the high temperature annealing step ensured that a carbon rich surface environment was maintained across the substrate. The gas-phase addition appeared to rectify non-uniformities associated with initial seeding.

(a)

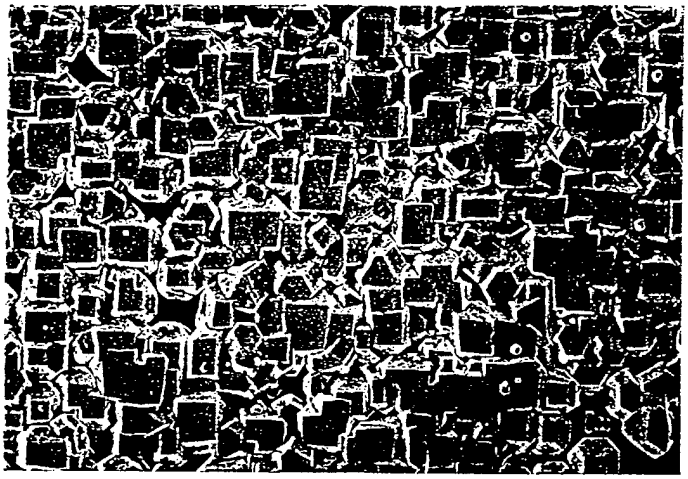

(b)

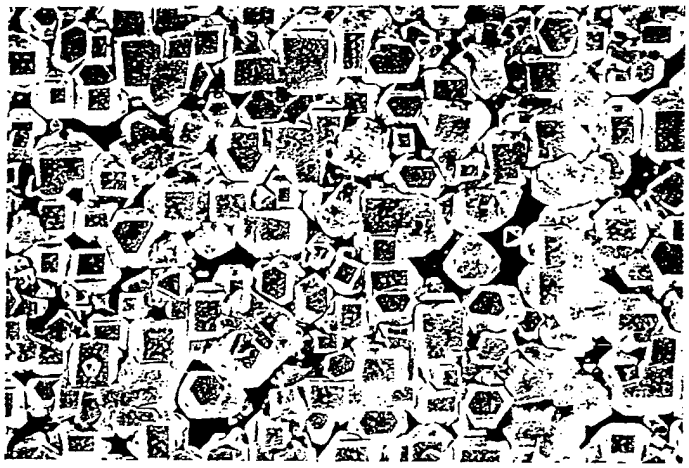

(c)

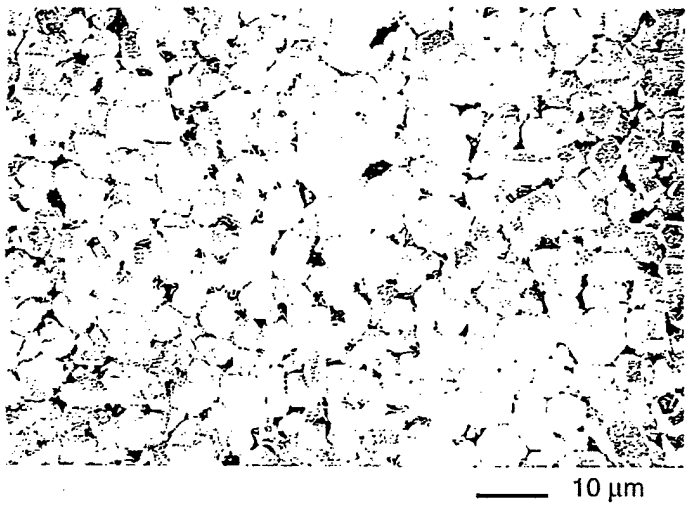

Figure 2. (100) oriented diamond on Ni obtained with different CH_4 concentrations in the high temperature annealing stage: (a) 0.5%, (b) 1% (c), 2.5%.

In order to produce a coalesced, oriented diamond film, a 49-hour growth was conducted in the hot filament CVD system. The pretreatment was carried out using seeding and 0.5% CH_4 in the gas phase. A polycrystalline, 1 mm thick Ni platelet was used as a substrate. The surface showed predominately (100) and (111) oriented grains on the order of several hundreds μm in size. A coalesced oriented diamond film was achieved across the substrate. Within each grain, the diamond deposit was found to be highly oriented. Because of the polycrystalline nature of the substrate, the orientation of each grain was slightly off the normal of the substrate, which lead to the growth steps observed in Figures 3a and 3b for (100) and

(a)

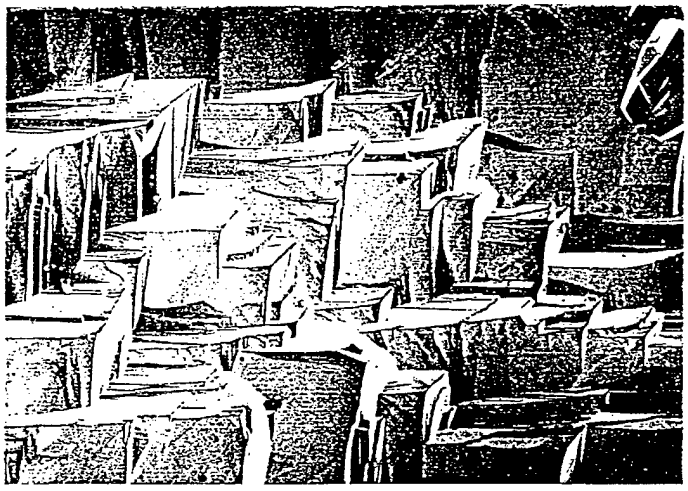

(b)

Figure 3. Coalesced oriented diamond films on (100) (a) and (111) (b) oriented nickel grains.

(111) grains, respectively. The coalesced diamond film was very uniform and about 30 μm thick. This thickness corresponded to a growth rate of 0.6 μm/hr. The phase purity of the grown diamond was evaluated by micro-Raman spectroscopy as shown in the insets of Figures 4a and 4b. Both crystal faces were found to be of high phase purity as indicated by sharp diamond signals at 1334 cm^{-1} with narrow peak widths ($FWHM_{100}$ = 5 cm^{-1},

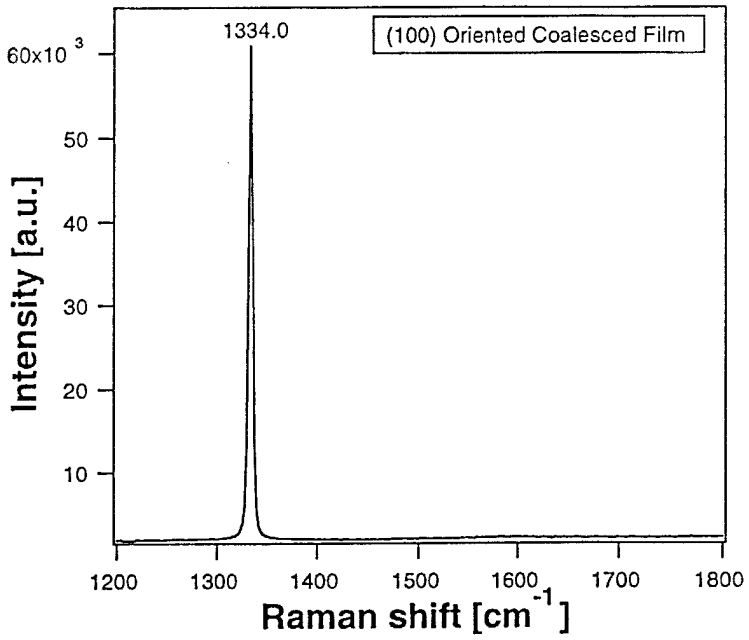

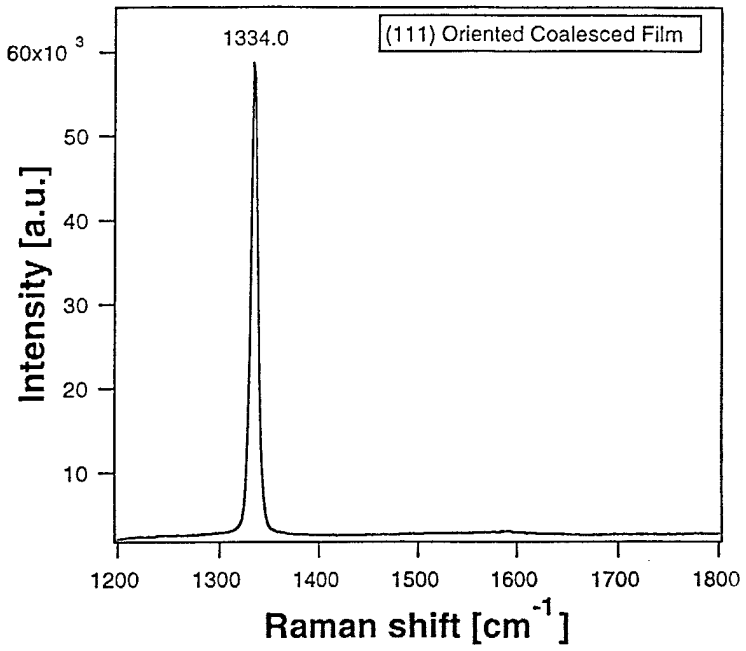

Figure 4. Raman spectra for (100) (a) and (111) (b) coalesced, oriented diamond films.

$FWHM_{111}$ = 8 cm^{-1}). The film delaminated and broke into a few pieces upon cooling. The fractures occurred primarily along the grain boundaries. In order to perform an x-ray pole figure measurement, as well as investigate thermal and optical properties, continuous, oriented diamond films will be grown on single crystalline Ni substrates using the same process parameters.

In conclusion, the Auger depth profile analysis revealed that at our annealing conditions carbon diffuses rapidly into nickel. In order to maintain a high carbon concentration at the surface, methane was introduced during the high temperature annealing. It was found that 0.5% CH_4 was optimal for both a high nucleation density and high degree of orientation, which are both important for the achievement of coalesced diamond films. Using the above nucleation procedure, high quality coalesced oriented diamond films were obtained after sufficient growth times. Micro-Raman measurements showed that both (100) and (111) oriented diamond films were of high quality with virtually no sp^2 bonded carbon present.

References

1. Y. Sato, H. Fujita, T. Ando, T. Tanaka, and M. Kamo, Phil. Transactions of the Royal Society of London **A342**, 225 (1993).
2. H.S. Dewan, D. Ravichandran, J.P. Cheng, W.R. Drawl, K.A. Cherian, and R. Roy, Proc of the Applied Diamond Conference 1995, Gaithersburg, MD, p.387.
3. T. Tachibana, Y. Yokota, K. Nishimura, K. Miyata, K. Kobashi, and Y. Schintani, Diamond and Rel. Mater. **5**, 197 (1996).
4. P.C. Yang, W. Zhu, and J.T. Glass, J. Mater. Res. **8**, 1773 (1993).
5. P.C. Yang, R. Schlesser, C.A. Wolden, W. Liu, R.F. Davis, J.T. Prater, and Z. Sitar, Appl. Phys. Lett. **70**, 2960 (1997).
6. M. Singleton and P. Nash, Bulletin of Alloy Phase Diagrams **10**, 2 (1989).

III. Properties of Nitrogen Doped Diamond Grown by Microwave Plasma Chemical Vapor Deposition

A. Introduction

Diamond has recently attracted much attention for use as a cold cathode material. Its excellent chemical stability and extreme hardness is ideal for cold cathode applications where minimal surface degradation is desired. In addition, with proper surface treatment, diamond surfaces have been shown to exhibit a negative electron affinity (NEA) [1]. An NEA surface occurs when the vacuum level lies below the conduction band minimum at the vacuum/semiconductor interface. The presence of an NEA means electrons in the conduction band can be emitted freely into vacuum. The ideal cold cathode material would then exhibit an NEA and sufficient n-type doping to supply electrons into the conduction band and to form low resistance contacts. To date, however, it has been proven difficult to produce n-type diamond.

Nitrogen has a high solubility in diamond and is found abundantly in natural single crystal stones. In these natural diamonds, nitrogen is present primarily in aggregate form. Nitrogen has also been found in synthetic diamond. Nitrogen in synthetic diamond is present predominantly as single substitutional atoms. Whether the nitrogen is present in aggregate or singly substitutional form in diamond can be determined by optical techniques. Singly substitutional nitrogen has been determined to be a deep donor in diamond at 1.7 eV below the conduction band [2].

Recent reports have indicated field emission from nitrogen doped diamond with threshold turn-on fields as low as 0.5 V/μm [3,4]. However, the mechanisms governing field emission from these samples and the role of nitrogen is still unclear. This report outlines the status of nitrogen incorporation in microwave plasma CVD diamond films and its influence on the properties of the films.

B. Experimental Procedure

Nitrogen-doped diamond films were deposited in a commercially available ASTeX HPMS stainless steel microwave (2.45 GHz) plasma CVD deposition chamber. *In situ* growth rate and film thickness information was monitored using laser reflectance interferometry (LRI) using the 632.8 nm line from a He-Ne laser at normal incidence and a Si photodiode as the photodetector. The conventional gas mixtures of hydrogen and methane were used as the growth precursors. Two sources of nitrogen were used depending on the desired nitrogen concentration in the process gas. For low nitrogen process concentrations, a mixture of nitrogen (2.11%) diluted in hydrogen was used. For high nitrogen concentrations, zero-grade nitrogen (99.998% minimum purity) was added to the process gas. With these two sources, nitrogen could be added as an impurity to the process gas with gas phase [N]/[C] ratios spanning from 0 to 80.

Polycrystalline diamond films containing nitrogen were deposited on 25 mm diameter n-type (1 Ω °cm) silicon substrates. In order to enhance nucleation, the substrates were hand polished for 10 minutes using 1-2 μm diamond grit applied to a nylon polishing cloth. The scratched wafers were then ultrasonically cleaned in acetone then methanol for 10 minutes in each solvent. After the solvent clean, the silicon wafers were blown dry with nitrogen gas. A two-step growth sequence was used to form the initial diamond nuclei and grow out the polycrystalline diamond films. Nucleation was achieved at 760°C surface temperature, 600 W microwave power, 20 Torr chamber pressure, and at a flow rate of 400 sccm using process gases consisting of 2 vol. % methane in hydrogen. Nucleation time was determined by monitoring the LRI signal for an initial drop in intensity. For most samples, the nucleation time was 21 minutes. Following the nucleation step, the substrate temperature, microwave power, and chamber pressure were increased to the growth conditions.

Nitrogen-doped diamond films were grown at substrate temperatures of 800–900°C, 1300 W microwave power, and 50 Torr chamber pressure. The growth process gases consisted of 0.5-2.0 vol. % methane and 0-12 vol. % nitrogen in hydrogen at a total flow rate of 500 sccm. Nitrogen was only added to the process gas during the growth step. Following deposition, the nitrogen-doped diamond films were characterized by micro-Raman spectroscopy, photoluminescence, optical microscopy, scanning electron microscopy (SEM), and field emission measurements.

The micro-Raman and PL spectra were recorded at room temperature with an ISA U-1000 scanning double monochromator using the 514.5 nm line of an argon ion laser as the excitation source. The laser beam was focused on the samples to a spot size of ~3 μm diameter using an Olympus BH-2 microscope.

The samples were examined using a Olympus BX60 microscope with magnifications up to 500× to identify large surface defects and/or damage both before and after field emission measurements. To evaluate the diamond film morphology and to distinguish smaller damage resulting from field emission measurements, the diamond thin films were imaged with a JEOL 6400 field emission SEM. This particular SEM was used for its high resolution capabilities at low accelerating voltages. Low accelerating voltages helped reduce charging effects while imaging diamond films.

Field emission measurements were obtained in an ultra-high vacuum (UHV) environment with pressures typically < 1×10^{-8} Torr. A cylinder of molybdenum (ϕ3 mm) was chosen as the anode for these measurements. The end of the cylinder was either polished flat or polished to a very high radius of curvature (typically > 5 mm) to minimize edge effects. The anode was mounted on a stage that was coupled to a UHV stepper motor. The stepper motor controled the distance between the anode and the sample. Current-voltage measurements were acquired with a computer-controlled Keithley 237 Source Measure Unit (SMU). The SMU can

simultaneously source a voltage and measure a current. A current limiting circuit was also included within the SMU so no voltage was applied that caused the current to exceed 1×10^{-7}A. This current limit was called the compliance value. A schematic of the field emission setup is shown in Fig. 1.

In any given measurement, a family of I-V curves was recorded with each curve corresponding to a different anode to sample spacing. Initially, the anode was positioned at some unknown distance above the sample. The stepper motor count was recorded and an I-V curve was collected. Next, the anode was moved closer to the sample by a fixed number of steps and the cycle was repeated until about 5-10 curves were collected. As expected, the current-voltage curves shifted to lower voltage values with decreased distance. Because of the nature of the Fowler-Nordhiem I-V equation, the "turn-on" voltage or critical threshold voltage must be defined in terms of a specific current value. The voltage that resulted in a current value of 10 nA was chosen to represent the critical threshold voltage for electron emission. This value was chosen because it was two orders of magnitude above the inherent noise and one order of magnitude below the compliance value. Next, each critical threshold voltage was plotted versus stepper motor count value, and as expected the resulting graph was linear. Upon fitting the data to a straight line, an average critical field for 10 nA of current wasobtained by dividing the slope of the line by the step size of the stepper motor (0.055 μm/step). This method for determining the average critical field did not rely upon the absolute anode to sample spacing, but rather the change in distance of the anode with respect to the sample.

C. Results

The focus of this work was the investigation of the role of nitrogen doping on the field emission properties of diamond. Efforts included the production of high-quality, nitrogen-

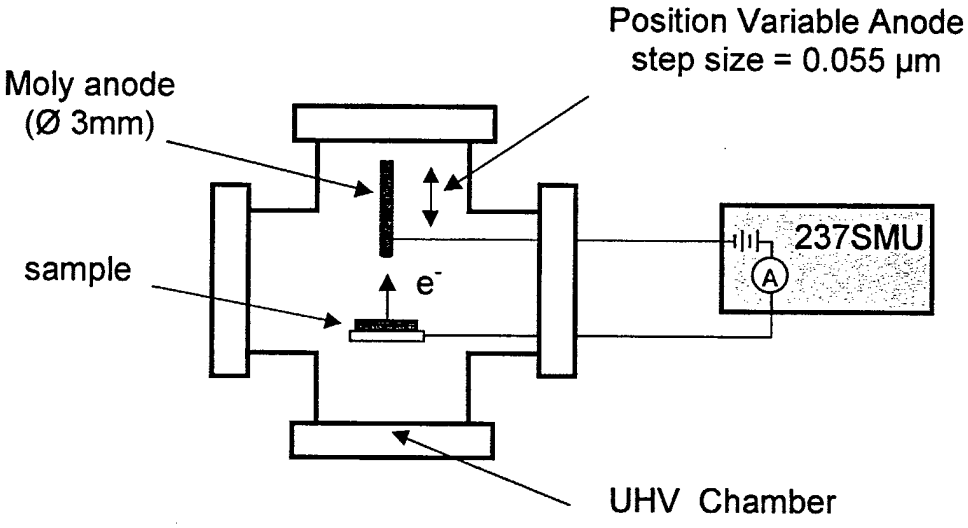

Figure 1. Schematic of the system used to measure field emission properties of thin films.

doped films without deliberately depositing highly defective films. Despite this objective, as seen below, adding nitrogen to the process gas directly affected the resulting film quality. In this study, over 30 nitrogen-doped samples were grown under various process conditions and for different film thicknesses.

Figure 2 shows the effect of nitrogen addition to the process gas on the growth rate of diamond films grown with 0.5 vol. % methane. Initially, very small nitrogen concentrations in the process gas greatly enhanced the growth rate by almost a factor of five. However, the addition of more nitrogen eventually led to a decrease in the growth rate. Ultimately, at [N]/[C] ratios of ~70, no deposition was observed and the substrates were visibly etched after being exposed to the plasma for a few hours. Similar results have been observed for samples grown with 2 vol. % methane, although data was not been collected for very high nitrogen concentrations.

Raman scattering spectra for the 0.5 vol. % methane series are shown in Figs. 3 and 4. Figure 3 corresponds to samples grown with [N]/[C] ratios of 0.1-1.0 while Fig. 4 represents films grown with higher nitrogen gas phase concentration ([N]/[C] ratios from 8-48). For reference, Fig. 5 is a Raman spectrum from a sample grown without nitrogen addition. The addition of even very small amounts of nitrogen led to a decrease in diamond film quality. Raman peaks associated with graphite at ~1350 cm^{-1} and ~1580 cm^{-1} were present in the spectra and became more prominent with increasing nitrogen content in the process gas. Other peaks from microcrystalline diamond and sp^2 bonding in diamond were also visible at

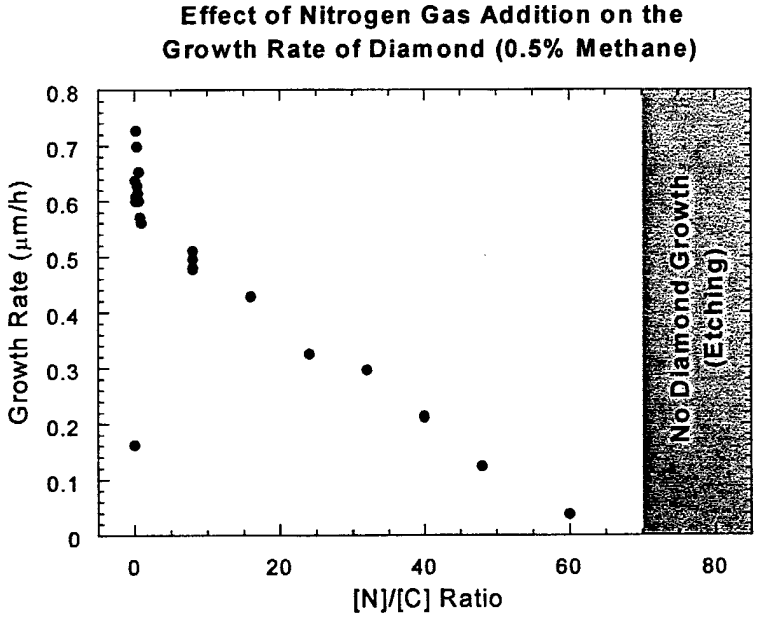

Figure 2. The effect of nitrogen gas addition to the process gas on the growth rate of nitrogen-doped diamond.

1120 cm^{-1} and 1500 cm^{-1}, respectively. As the nitrogen content in the process gas was increased to higher concentrations, as shown in Fig. 4, other features were present in the Raman spectra. Most notably was the presence of two peaks at 1190 cm^{-1} and 1550 cm^{-1}. One possible origin of these peaks might have been from N-C complexes in the films, although more work needs to be performed to determine their identity. The peaks associated with graphite, sp^2 bonding in diamond, and microcrystalline diamond were all reduced in intensity as the nitrogen addition was increased in this sample series. The FWHM of the diamond peak versus nitrogen process gas content for all Raman spectra in Figs. 3-5 is shown in Fig. 6. The FWHM of the diamond peak increased steadily initially, but saturated at ~15 cm^{-1} at a gas phase [N]/[C] ratio of 1.0.

Under certain process conditions at ~900°C, nitrogen-doped diamond films were deposited which exhibited PL bands attributed to nitrogen+vacancy optical centers. These bands were a characteristic of single substitutional nitrogen doping in diamond seen in type Ib HTHP synthetic diamond. The PL spectra for several nitrogen-doped diamond samples exhibiting this luminescence is shown in Fig. 7. These two nitrogen related bands were found at 1.945eV and 2.154eV. Nitrogen addition to the process gas also enhanced the 1.680eV band that had been attributed to silicon incorporation in diamond films.

The initial field emission experiments were performed to determine whether there was an optimum film thickness for the emission properties of nitrogen doped diamond. For these experiments, nitrogen-doped diamond was deposited with 0.5 vol. % methane and [N]/[C]=0.25. Films with thickness ranging from 0.13 to 6.0μm were grown and their field emission characteristics measured. Figure 8 illustrates the dependence of the threshold field upon the film thickness. The 0.13 and 0.75μm films had the best threshold field, but were more susceptible to damage and arcing. As a result, a film thickness of ~1μm was chosen for further field emission studies to minimize surface damage. Subsequently, several nitrogen-doped films were grown under varying conditions. No significant correlation between process parameters and field emission characteristics was observed for these samples. All 1μm thick films grown with 0.5-2.0 vol. % methane and [N]/[C] gas phase concentrations from 0.1 to 8.0 exhibited threshold fields around 70-90V/μm.

D. Discussion

It has been reported for diamond, in general, that lower threshold fields are obtained for films with higher defect densities [6]. The objective of this work was to grow high-quality, nitrogen-doped diamond films and to determine the role of nitrogen in these films. However, as seen above, the diamond film quality was diminished by even small nitrogen concentrations in the process gas. The field emission properties of films with [N]/[C] gas phase concentrations up to 8 were measured. Despite the decrease in film quality, there did not appear

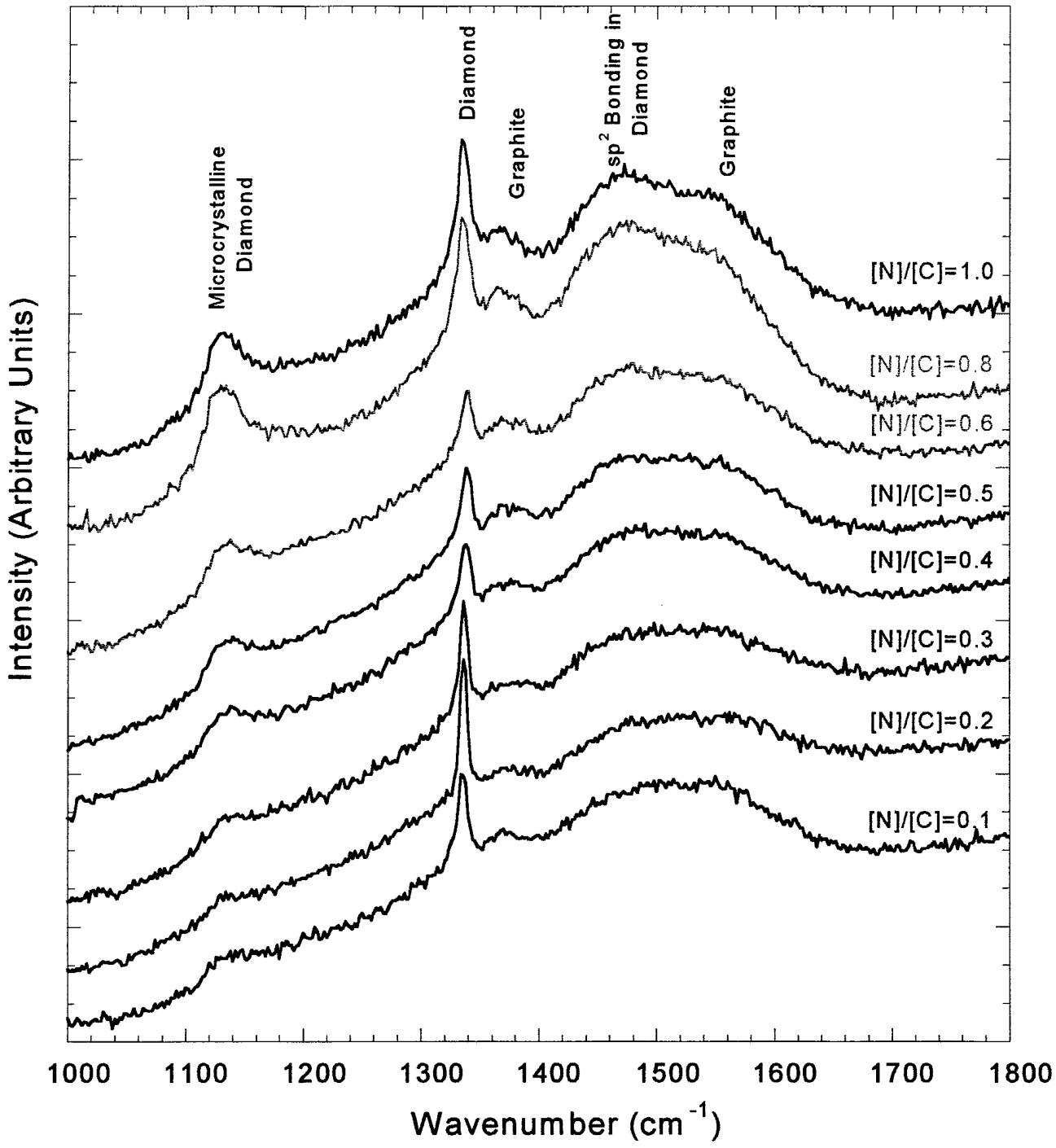

Figure 3. Raman scattering spectra from nitrogen-doped diamond grown with [N]/[C] gas phase ratios from 0.1 to 1.0.

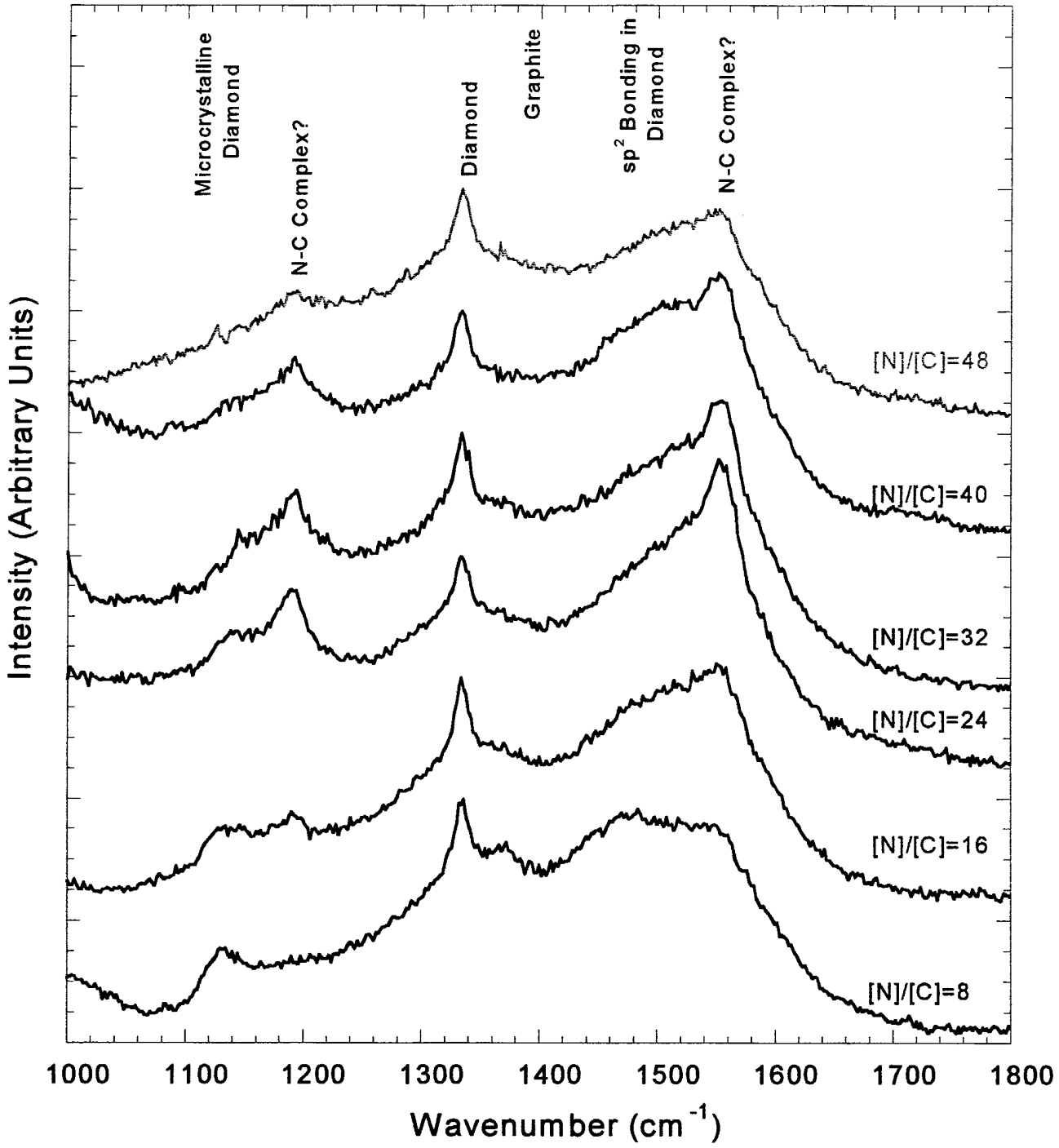

Figure 4. Raman scattering spectra from nitrogen-doped diamond grown with [N]/[C] gas phase ratios from 8 to 48.

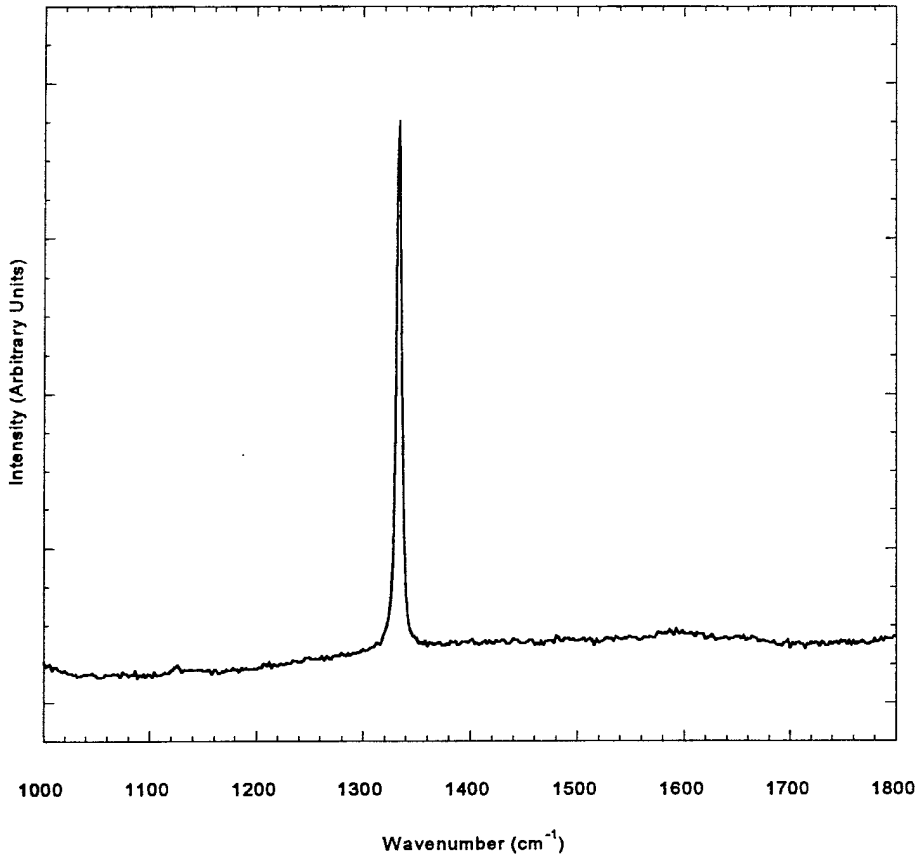

Figure 5. The Raman spectrum of a diamond film grown without nitrogen addition.

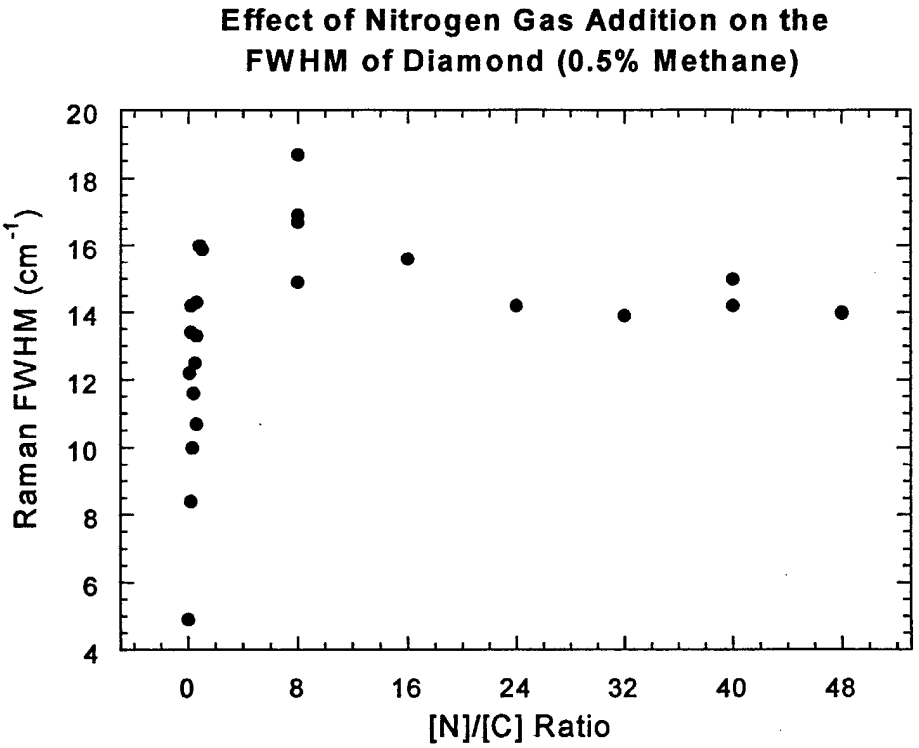

Figure 6. The FWHM of the diamond peak versus nitrogen process gas content for nitrogen doped films grown with [N]/[C] ratios from 0 to 48.

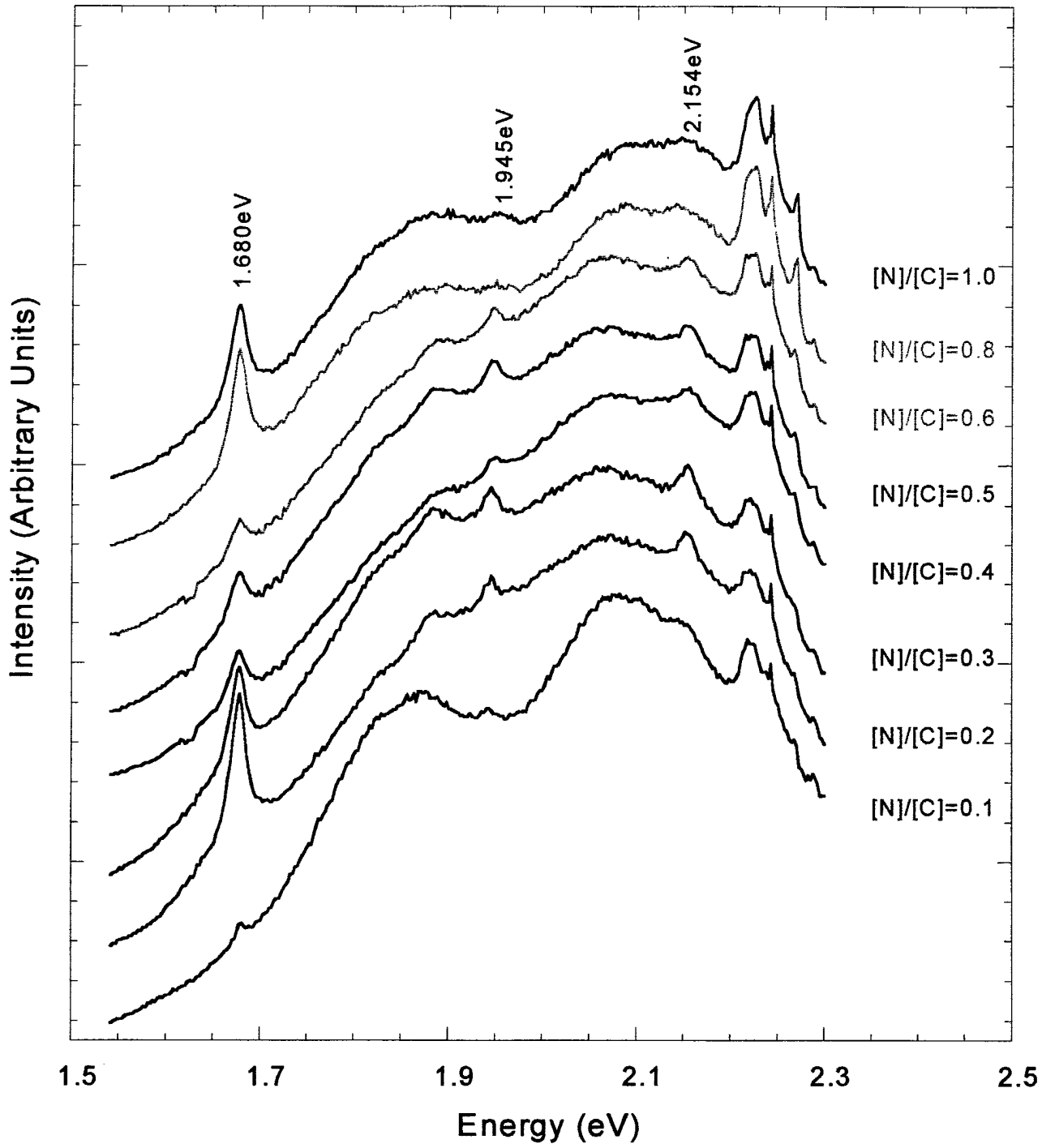

Figure 7. Photoluminescence spectra from nitrogen-doped diamond grown with [N]/[C] gas phase ratios from 0.1 to 1.0.

to be an improvement in the field emission properties. A possible explanation for this behavior could be that the nitrogen was completely compensated by defects. The resulting film in which the nitrogen atoms did not participate electrically would act like a simple dielectric. Two possible models for electron emission from these materials are shown in Fig. 9. In both models, the field was dropped across vacuum and the nitrogen-doped diamond with the field in the film reduced by the dielectric constant. In Fig. 9a, electrons in the silicon tunnel into the conduction band of the diamond were emitted into vacuum. In Fig. 9b, electrons were emitted from conducting defect states located in the band gap at the Fermi level. At this point, it was unclear which mechanism correctly described the field emission process from these films. Energy analysis of the electrons emitted from these films would be able to identify the appropriate process.

E. Conclusions

Nitrogen-doped diamond was deposited by microwave plasma using nitrogen gas as the dopant source. LRI data showed that the diamond growth rate initially increased for small nitrogen addition but fell off linearly with high [N]/[C] gas phase ratios. Under very high nitrogen concentrations in the process gas, no deposition was observed and the substrates were visibly roughened. Raman scattering spectroscopy indicated a decrease in film quality with nitrogen doping. Features possibly attributed to N-C complexes were observed in the Raman

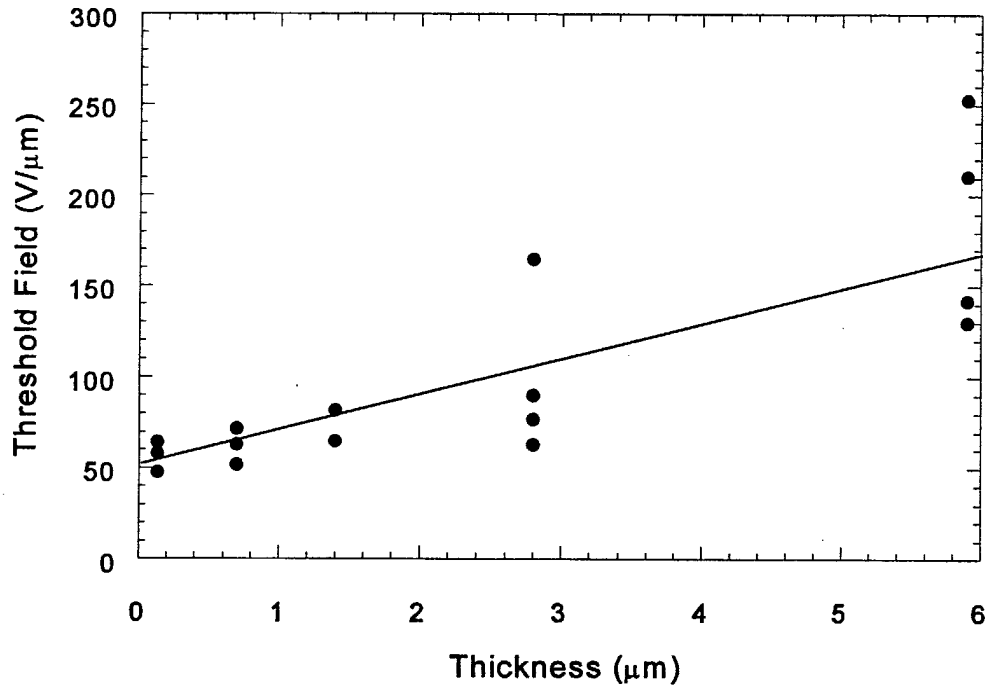

Figure 8. Influence of the film thickness on the threshold field characteristics of nitrogen doped diamond films. These films were grown with 0.5 vol. % methane and [N]/[C]=0.25.

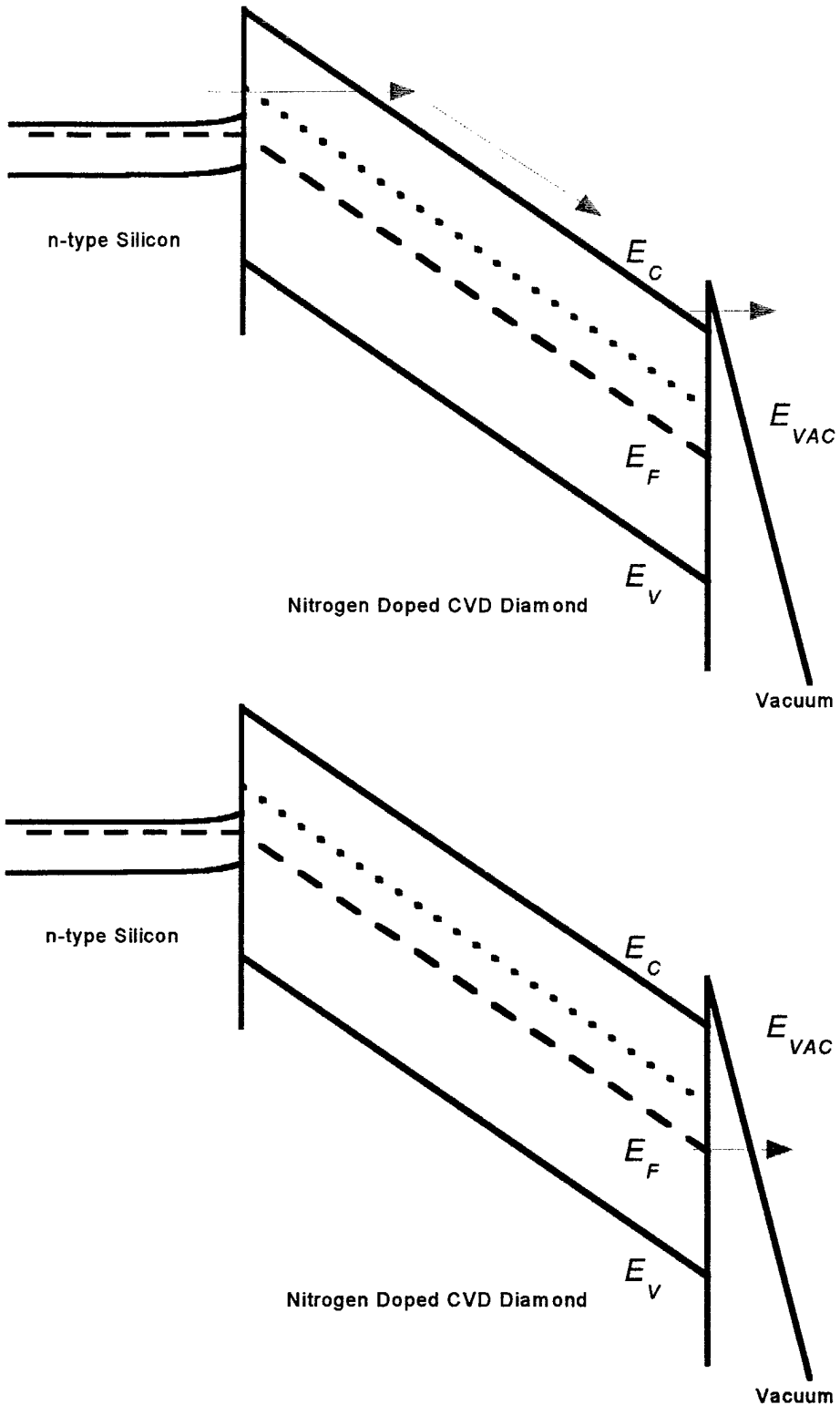

Figure 9. Schematics of the energy bands of nitrogen-doped diamond showing two possible mechanisms for electron emission.

spectra for higher [N]/[C] levels. At higher substrate temperatures, photoluminescence bands attributed to single substitutional nitrogen were present in the PL spectra. Field emission measurements indicated threshold fields of 70-90 V/μm independent of process conditions. Two models for electron from these materials were presented. One model suggested emission from the conduction band of the nitrogen doped diamond, while the other employed defect states in the gap as the source of emission.

F. References

1. J. van der Weide, Z. Zhang, P.K. Baumann, M.G., Wensell, J. Bernholc, and R.J. Nemanich, Phys. Rev. B **50**, 5803 (1994).
2. R.G. Farrer, Solid State Commun. **7**, 685 (1969).
3. K. Okano, S. Koizumi, S. Ravi, P. Silva, and G.A.J. Amaratunga, Nature **381**, 140 (1996).
4. M.W. Geis, J.C. Twichell, N.N. Efremow, K. Krohn, and T.M. Lyszczarz, Appl. Phys. Lett. **68**, 2294 (1996).
5. W. Zhu, G.P. Kochanski, S. Jin, and L. Seibles, J. Appl. Phys. **78**, 2707 (1995).

IV. Electron Emission from CVD Diamond Cold Cathodes

Peter K. Baumann [a] and Robert J. Nemanich [b]

[a] Materials Science Division, Argonne National Laboratory, Argonne, IL 60439, USA

[b] Department of Physics, North Carolina State University, Raleigh, NC 27695-8202, USA

15.1 Abstract

This review focuses on electron emission from diamond. The electron affinity is a measure of the barrier to emission of electrons from the conduction band into vacuum. The effect of surface properties on the electron affinity of semiconductors is described in terms of the surface dipole. In particular, it is shown that surface adsorbates can affect the electron affinity of diamond, and hydrogen leads to a negative electron affinity while oxygen termination and adsorbate free surfaces exhibit a positive electron affinity. Thin metallic layers can also lead to an effective negative electron affinity of diamond and some surfaces are stable to ambient air exposure. Field emission is a more complicated process that appears to be due to electrons in the valence band or from defects in the gap. Yet, the field emission is dependent on the surface termination.

15.2 Introduction

Electron beams are fundamental to many electronic applications ranging from cathode ray tube (CRT) displays to microwave or power amplifiers. While hot cathodes are suitable for many applications, the development of cold cathodes could lead to improved performance in many existing applications and, more importantly, to new technologies including vacuum micro-electronics, flat panel display technologies and new types of microwave amplifiers. A new approach being considered for these applications is to employ semiconducting materials in which electrons in the conduction band can be emitted directly into vacuum without overcoming an energy barrier. This property of the semiconductor has been termed a negative electron affinity (NEA).

The first evidence of this possibility was reported for diamond. Himpsel et al. [1] and Pate [2] reported a high quantum efficiency for photoelectron emission from (111) surfaces of natural diamond samples. It was concluded that these surfaces did indeed exhibit a true negative electron affinity, and hydrogen termination was found to induce induce this effect on the (111) surface. These studies first highlighted the potential of diamond as a cold cathode source material.

As diamond film deposition techniques have been developed since the first photoemission studies, there has been substantial interest in studying the potential of diamond as the emitting material in electron emission structures and devices.

Cold electron emission from metals by means of high electric fields (i.e. field emission) has been studied for many years.[3] And it has been known that low workfunction metals emit electrons more readily that metals with a higher workfunction. The emission process for a semiconductor is more complicated than for a semiconductor. Considering a semiconductor electron emission structure, electrons must be supplied to the semiconductor and then extracted with by an electric field at the surface. The field emission

process then involves, injection of electrons from an electrical contact into the semiconductor, transport of the electrons through the bulk to the emitting surface and finally the emission from the surface into vacuum. The initial studies of Himpsel et al. [1] and Pate [2] demonstrated that unlike metal surfaces, the emitting surface will not limit the emission for hydrogen terminated (111) natural diamond surfaces.

In this report recent studies pertaining to electron emission based on diamond are reviewed. The relation of the electron affinity to the surface properties is presented. The determination of the electron affinity by means of photoemission and secondary electron emission is described. Results for diamond surfaces are reported. Since field emission will be required for most device applications, representative measurements are presented. The complexity of the measurements are discussed.

15.3 Electron Affinity and Negative Electron Affinity

15.3.1 Definition of Electron Affinity and Negative Electron Affinity

The electron affinity of a semiconductor is defined as the energy difference between the vacuum level and the conduction band minimum both extrapolated to the surface. This corresponds to the energy necessary to excite an electron from the conduction band minimum to the vacuum. We also note that the vacuum level is the energy of an electron at rest in vacuum. The free electron model essentially describes the band structure of the vacuum. It is probably worth noting that the electron affinity of the semiconductor is essentially the heterojunction band offset between the semiconductor and vacuum.

In general, the electron affinity is independent of the position of the Fermi level. We make this point since the work function of semiconductors are sometimes quoted, but in general, the work function may be different for p- and n-type doping. For most

semiconducting materials the vacuum level lies above the conduction band minimum, and by convention this has been defined as the electron affinity. For wide bandgap semiconductors like diamond, the conduction band minimum will be near to the vacuum level. And in fact in some instances the vacuum level is below the conduction band minimum. This case has been termed a negative electron affinity or simply NEA. In this case electrons present in the conduction band have sufficient energy to overcome the workfunction of the surface and can be emitted into vacuum.

There are many ways to view the energetics of a semiconductor surface, but the following is helpful in understanding some effects to be described here. The electron affinity of a semiconductor may be determined by (1) the properties of the material itself as well as (2) the surface termination including adsorbates, reconstructions and steps.[4] A schematic illustrating of these effects is shown in Fig. 1.[5] The atomic levels essentially reference the ionization energy of the atom to the levels that broaden into the valence band. Since the atomic levels are more or less intrinsic to a material, they cannot be changed (but alloys may provide a degree of variation). At the surface of any material effects can lead to the formation of a surface dipole. {We note that it is difficult to define the surface dipole exactly, but in much of what follows we will examine how various processes increase or decrease the value of the surface dipole.} For a simple free electron metal, the surface dipole would arise from the quantum mechanical extension of the electron wavefunctions into the vacuum beyond the surface. This also results in a positive layer due to the loss of this electron density. The combination of the electron density away from the surface with the positive charge layer results in a surface dipole that effectively holds electrons in the material.

However, the surface dipole can be influenced substantially by surface adsorbates, surface reconstructions and steps on the surface. These effects may either increase or decrease the electron affinity of the semiconductor. Ignoring the specifics of bonding and

charge distribution, a molecular adsorbate that pulls electrons from the surface towards the adsorbate will increase the electron affinity while an adsorbate that contributes electrons to the material will result in a lower electron affinity.

To illustrate the magnitude of this effect consider a hydrogen passivated surface. Let's assume that the average nuclear and electronic charges are point charges separated by 0.5Å. Then for a surface density of $1x10^{15}cm^{-2}$ a surface dipole induced energy shift of about 9 eV can be calculated. (Certainly complete charge transfer is never a reasonable possibility, but this simple calculation demonstrates the significance of the surface dipole.) Full quantum mechanical calculations have addressed the properties of the H terminated diamond surface, and they will be mentioned below. Since the effect of the surface dipole is so large, it is basically impossible to determine if a material is "intrinsically NEA." Thus the surface termination is critical in describing the electron affinity (or NEA) properties of a material.

15.3.2 Techniques

While UV-photoemission measurements first detected the high quantum efficiency of electron emission, the technique of UV-Photoemission spectroscopy (UPS) is a very sensitive method to determine whether a surface exhibits a NEA or to measure the positive electron affinity.[1,2] In this technique, the incident light excites electrons from the valence band into states in the conduction band. Some of these electrons quasi - thermalize to the conduction band minimum. For NEA surfaces these secondary electrons may be emitted into vacuum and are detected as a sharp feature at the low energy end of photoemission spectra. A careful measurement of the width of the photoemission spectrum can be used to determine if the low energy emission occurs from the conduction band minimum. The width represents the energy difference from the photoemission onset to the low energy

cutoff. For a positive electron affinity the low energy cutoff will be determined by the vacuum level, and emission from the conduction band minimum will not be detected. A schematic of photoemission spectra of a semiconductor with a NEA or a positive electron affinity is shown in Fig. 2.[6] The electron affinity (χ) or the presence of a negative electron affinity can be deduced from the width of the spectrum (W) as follows:

$$\chi = h\nu - E_g - W \quad \text{for a positive electron affinity} \qquad (1)$$
$$0 = h\nu - E_g - W \quad \text{for a negative electron affinity}$$

where $h\nu$ is the photon energy and E_g is the bandgap. It is evident that for a positive electron affinity, the value of the electron affinity can be deduced from the measured width of the spectrum. It needs to be emphasized, however. that the absolute value of the electron affinity for a NEA surface cannot be measured by means of photoemission spectroscopy.

By carefully measuring the spectral width one can determine whether the low energy emission originates from the conduction band minimum. In fact recent measurements have indicated emission that extends several tenths of an eV below the conduction band minimum. Bandis and Pate have ascribed this emission to excitons for the C(111) surface exhibiting a NEA.[7] It was found that the observation depended on the band bending near the surface. For flat band and upward band bending, exciton emission was observed while for downward band bending the emission was ascribed to electrons in the band.[7] The band bending may be due to states in the bandgap that cause Fermi level pinning. Another possibility is H passivation of the boron acceptors near the surface which will lead to different band bending for the different regions on the surface.[8]

Photoemission spectroscopy can also be used to determine the position of the surface Fermi level. For a grounded sample, the Fermi level of the sample will be the same

as that of the metal sample holder. And the Fermi level of the metal can easily be determined. This measurement can be employed to monitor the semiconductor Fermi level or to detect band bending. We note that care must be taken to avoid photovoltage shifts that may be observed in highly resistive samples.

Secondary electron emission (SEE) is another technique that can also be used to characterize the surface.[9,10,11] To facilitate the secondary emission experiments, the sample is exposed to a monochromatic source of high energy electrons. Typically accelerating voltages are 1-5kV. Electron-hole pairs are generated in the conduction and valence band of the semiconductor by the incident electrons. The electrons then move toward the surface and may be emitted as described in the photoemission process. In general, SEE is less surface sensitive than UPS, since the electrons generated in SEE are distributed deeper in the sample than those from UPS. A typical application of this technique is to measure the electrons emitted per incident electron. We note that the gain is obtained since a single high energy electron can excite numerous electron-hole pairs that can be emitted and detected. A negative electron affinity surface will enhance the emission of electrons.

An alternative measurement is to obtain the energy spectrum of the emitted electrons. Similar to photoemission spectra, a negative electron affinity would be indicated by the presence of a sharp low energy peak in the SEE spectra (corresponding to the one displayed in Fig. 2). The energy of the incident electron beam depends on the work function of the electron gun relative to that of the target material. This effect makes an analysis based on a measurement of the width of the spectrum more difficult than for UPS.

It also needs to be emphasized that since the electron-hole pairs are excited deep in the sample in comparison to UPS any band bending at the semiconductor surface is going to influence the SEE gain. In particular, an upward band bending will inhibit electron transport to the surface while a downward band bending will sweep electrons towards the

surface. Therefore UPS is more suitable and easier to use than SEE to determine the electron affinity of a semiconductor surface.

15.3.3 Surface Termination Effects due to Molecular Adsorbates on Diamond

Different surface terminations can shift the position of the bands with respect to the vacuum level and, therefore, induce a NEA or remove it. Such changes have been found for molecular surface adsorbates. Different molecular surface adsorbates result in changes of the surface dipole layer, and for a wide bandgap material the surface dipole layer can lead to a positive or negative electron affinity. For example hydrogen has been reported to induce a NEA on the diamond (111) surface.[1,2,6,12] More recently a NEA effect has been shown for the hydrogenated C(100) and C(110) surfaces.[8,13,14,15] In comparison oxygen leads to a dipole such that a positive electron affinity is observed on these surfaces.

Various surface treatments designed to remove non-diamond carbon result in an oxygen terminated surface. These include acid etching and an electrochemical etch process. It has been suggested that different treatments can lead to different bonding configurations (bridge - versus double bonding) of oxygen on the C(100) surface.[8,16,17] Vacuum annealing of cleaned C(100) to 500°C does not remove a significant portion of the oxygen from the surface as detected by means of Auger electron spectroscopy (AES) indicating that most of the oxygen was chemisorbed. The UPS spectra of as-loaded samples as well as those heated to 500°C showed a positive electron affinity. A value for the electron affinity of 1.5 eV was detected following the 500°C anneal. Following an anneal to about 1000°C the amount of oxygen on the surface dropped below the detection limit of the AES instrument. A reconstructed (2x1) LEED pattern appeared. In addition, the width of the

UPS spectra increased to ~ 15.7 eV, and a sharp low energy feature appeared indicating a NEA following the last annealing step. It was presumed that the surface was hydrogen terminated after this step.

Annealing the (100) surface to greater than 1150°C results in the desorption of the remaining hydrogen, and a clean surface is obtained that exhibits a 2x1 reconstruction. The UPS measurements of this surface display a positive electron affinity. Fig. 3 shows UV photoemission spectra for oxygen terminated, clean and hydrogen terminated diamond (100) surfaces. The NEA character of the H-terminated surface is evident in both the width of the spectrum and the presence of the sharp peak at the lowest binding energy.

Further hydrogen plasma exposed surfaces exhibited a NEA and 2x1 reconstruction indicating a monohydride termination. These studies were actually preceded by ab initio calculations suggesting a NEA for the monohydride terminated 2x1 reconstructed (100) surface [13]. The same theoretical studies reported a positive electron affinity for the clean 2x1 surface in agreement with experimental observations. In fact the difference in the electron affinity between the two surfaces was ~3eV indicating the magnitude of the change in the surface dipole.

Diamond (110) surfaces also exhibited oxygen termination after surface cleaning, and they were found to have a positive electron affinity as evidenced by means of UPS.[8] Subsequent to annealing the samples to 700°C, the oxygen concentration on the surface dropped to below the detection limit of the AES instrument. The low energy cut off of the UPS spectrum shifted to lower energies, indicating a reduction of the electron affinity. In addition, a sharp low energy peak attributed to a NEA appeared. A 800°C anneal removed the sharp NEA feature, and the width of the spectrum was reduced by 0.7 eV. Exposing the surfaces to a H plasma resulted in the re-appearance of the NEA characteristics. Employing a 800°C anneal the NEA could be removed again. The results for the (100) and (110) hydrogen terminated, oxygen terminated and clean surface are summarized in Table

1.

In Fig. 4 a schematic of the band alignments for a clean and hydrogen terminated diamond surface is shown, with band bending consistent with p-type doping. Hydrogenation changes the surface dipole layer. This causes a shift of the bands with respect to the vacuum level. Overall, oxygen is bonded the strongest to diamond (100) - and the weakest to diamond (111) surfaces, and the bond strength of O on the C(110) surface falls between these two values.[8] Following this approach, according to the annealing temperatures necessary to remove a NEA from a hydrogen terminated diamond surface, the hydrogenation of the diamond (100) surface appears to be the most stable while that of the (110) the least thermally stable, while C(111) falls in-between.[8]

Recent work has explored the effects and stability of deuterium bonding on diamond. Deuterium termination has been found to induce a NEA effect comparable to hydrogen, but the surface was stable to a higher temperature than a hydrogen terminated surface. Future studies should focus on the stability of the hydrogen or deuterium terminated surfaces and the interactions with oxygen.

15.3.4 Metallic and Oxide Layers on Diamond

Deposition thin films of metal is another possibility of inducing an effective NEA on diamond. It has been known for many years that low workfunction metals like Cs can induce NEA type characteristics on III-V semiconductors like GaAs. High efficiency photocathodes are based on such structures. Cs deposition on diamond has also been demonstrated to induce a NEA effect.[18,19] Since diamond has a large bandgap other, higher workfunction metals may be suitable to establish a NEA. A few years ago Ti [20] or Ni [21] have been found to induce a NEA on diamond (111). More recently NEA characteristics have been reported for Co, Cu or Zr on diamond (100), (111) and (110)

surfaces.[16,22-24] Fig. 5 shows a summary photoemission spectra of diamond surfaces coated with a few monolayers of these metals. A sharp peak indicative of a NEA is detected for all these spectra.

Deposition of a thin metal layer was found to change the effective electron affinity of the diamond surface. This effect is illustrated in Fig. 6 for Ti on the clean diamond surface. This structure was found to exhibit a NEA. The effective electron affinity for a thin metal layer on the diamond can be modeled in terms of two interfaces: the vacuum-metal and the metal-diamond. Equation (2) gives an expression for the effective electron affinity.

$$\chi_{eff} = (\Phi_M + \Phi_B) - E_G \qquad (2)$$

In this model a lower Schottky barrier height would result in a lower effective electron affinity, and this is consistent with the experimental results. For each metal the surface termination prior to metal deposition appears to be have a significant effect on the Schottky barrier height. For metals deposited on clean surfaces lower values for the Schottky barrier height and a greater likelihood of inducing a NEA are expected than for metals on non adsorbate free surfaces. Fig. 7 shows the band diagrams for Ti on a clean or a H-terminated diamond surface. Metal - diamond interfaces exhibiting a NEA have a lower Schottky barrier height than those exhibiting a positive electron affinity.

In Fig. 8 the experimentally (by means of UV photoemission) measured Schottky barrier heights are plotted vs. the metal workfunction.[24] It is indicated whether a NEA or a positive electron affinity was observed by means of UV photoemission. The experimantal data are also compared to equation (2).

Of the results obtained to date the most significant may be the observation of a NEA of Co and Zr on diamond (100), (111) and (110).[23,24] These films have been shown to

be uniform with little tendency to the islanding that has been observed for Ni and Cu.[23,25] It has also been demonstrated that the NEA was stable following air exposure for Cu, Co and Zr on diamond surfaces.[23,24] It has also been demonstrated that Ti-oxide induces a NEA on diamond (111) surfaces.[26]

15.4 Field Emission

15.4.1 Description of Field Emission Process

Most practical applications of electron emitters will require field induced emission. The actual field emission process from a semiconductor combines four effects (1) electron supply to the semiconductor, (2) transport through the semiconductor, (3) emission into the vacuum and (4) transport in vacuum to the anode. For an ideal structure with a negative electron affinity and a low resistance contact and semiconductor, the electron emission would be limited by space charge in the vacuum, the I-V characteristics would exhibit a $V^{3/2}$ dependence. For the case of a positive electron affinity and low resistance contact and semiconductor, the material would essentially respond as a metal and Fowler-Nordheim characteristics would be obtained. For an intrinsic semiconductor with a negative electron affinity the emitted current would be limited by electron injection into the semiconductor, and since this may be a tunneling process, Fowler-Nordheim characteristics may also be obtained. In this situation the current could also be limited by space charge effects in the semiconductor.

Field (electron) emission is not only a promising means to develop intense/controlled electron currents for a variety of devices. It is also a powerful and rapid research tool to study the mechanisms of electron emission, whatever the means of stimulation.

15.4.2 Techniques

The field emission characteristics of diamond surfaces are most commonly determined by using either a movable probe as an anode that can be stepped toward the surface of the specimen [23,27,28], a large flat anode kept at a certain distance (typically in the mm range) away from the sample by a spacer [29,30,31] or a probe that is used to scan across the surface.[31,32] In the case of a movable anode the current voltage characteristics are measured at different distances. The distances are of the order of a few μm to a few 10 μm. To avoid emission from edges of the anode it often has a spherical shape with a diameter of a few mm. This method has the advantage that the emission can be determined as a function of distance which may be important for the characterization of rough or highly resistive samples. The technique employing the large anode has the advantage of exploring the entire surface area. Also if a fluorescing anode is used, the location of various emission sites can be observed. However in this method field emitted electrons with KeV energies are striking the anode and can desorb material from there. In turn the cathode is exposed to KeV energy ions from the anode. As a result the surface of the cathode gets contaminated and discharges can occur. These effects can lead to changes in the emission behavior. Also when employing a phosphor screen as an anode problems can occur since small amounts of phosphor powder may get pulled to the cathode due to the high electric fields. Using a concentrated binder with the phosphor may alleviate this problem. To avoid the problems with phosphor an indium tin oxide (ITO) layer can be used instead.[30] But a higher voltage is necessary for ITO, increasing the likelihood of changing the emission characteristics due to contamination of the cathode surface or the striking of a discharge. Also the spatial resolution of an ITO coated anode is worse due to the higher energy of the electrons hitting the anode. Overall, to avoid discharging effects, a

better vacuum needs to be maintained for the technique using a large anode kept at a large distance, than for a method employing a probe in close proximity of the emitting surface. A variation of this technique is the arrangement of an anode grid close to the surface facilitating the field emission. A collector screen can then be placed at a larger distance away from the sample surface.[31] The third technique employs a tip that is placed a few μm from the emitting surface and can be scanned across this surface. This method can be useful for correlating the distribution of emission sites with the surface morphology.

15.4.3 Field Emission Results from Diamond

There have now been several studies that indicated electron emission from flat diamond surfaces at relatively low fields. Kordesh and co-workers used field emission microscopy and showed a uniform emission from p-type diamond films at low fields (~3V/μm).[33] Using a scanning probe with μm resolution Talin et al. reported turn on fields of 3V/μm for about 1/2 of the surface area of nanocrystalline diamond.[32] Raman spectra of the emitting areas exhibited lower quality sp^3 bonding. Latham and co-workers also measured field emission from flat diamond films at fields of ~20V/μm. They also showed that the emission was from very specific point sites that may be correlated with defect structures rather than sharp features of the films.[34] Zhu and co-workers found a correlation with specific sp^2 bonding structures in the films.[28,35] As shown in Fig. 9 higher electric fields were necessary for emission from high quality p-type diamond than for defective or particulate diamond.[35] To date, most of these measurements were on p-type boron doped diamond. Miskovsky and Cutler have analyzed the emission possibilities from these films and suggested that states in the bandgap must be present and participate in the emission process to account for the low field emission from the p-type material.[35,36]

It has been found that thin metal films of Cu, Co, or Zr on natural crystal p-type

diamond resulted in a decrease in the field emission threshold compared to the oxygen terminated diamond surface. The results of the field emission threshold and electron affinity showed a similar trend in which the field emission threshold decreased as the electron affinity decreased.[36,37]

Prins has developed a method of ion implanting diamond to produce nominally n-type material.[38,39] Geis and co-workers have used this technique to fabricate a diamond cold cathode emitter structure based on an all diamond p-n junction.[40] Carbon ion implantation was employed to induce the n-type like characteristics in diamond. Fig. 10 shows a schematic of the cold cathode device.[40] The diode current vs. applied voltage for the carbon ion implanted diode was compared to that of an aluminum Schottky contact on p-type diamond. Fig. 11 illustrates the measured I-V characteristics for both structures.[40] Geis et al. have also obtained field emission from nitrogen doped diamond.[27] There are several possible configurations for nitrogen impurities in diamond, but for nitrogen occupying single substitutional sites, the impurities exhibit n-type characteristics with a donor level at ~1.7eV below the conduction band. These materials also showed low field emission, but the spatial variation has not been reported.

There have also been several recent studies of the field emission from diamond coated field emitters (i.e. pointed structures) made of silicon or metals.[33,41-46] In these measurements the electron emission was found at significantly lower fields than from uncoated surfaces. However many studies have shown nonuniform growth of CVD diamond on the sharp tips. In particular, distinct diamond particles have been observed on the tips as shown in Fig. 12.[47] Possible explanations for the electron emission based on negative electron affinity diamond surfaces or based on different radii of silicon tips underneath the diamond have been proposed.[46,47] The growth of nanocrystalline CVD diamond has been reported.[32,48-50] This material may be suitable for coating field emitter tips (or flat emission surfaces) with a smooth, uniform diamond layer. Preliminary

results of emitter tips coated with nanocrystalline diamond indicate a significant (3-fold) reduction in field emission threshold compared to the uncoated tips.[51]

It is evident that the complicated processes involved in field emission have impeded the advancement of our understanding of these measurements. The measurements themselves require care, and in fact, some early reports may have been dominated by artifacts attributable to poor vacuum or other effects due to the high fields present in the measurements. The residual gas in the measuring chamber results in a background ion current. Moreover the strong fields can sometimes cause a plasma to ignite and severely damage the surface. Following arc discharges, crater formations and molten areas with debris were observed in the surface of CVD diamond and amorphous carbon films.[52] A corresponding improvement in the field emission has been reported. It has been suggested that this improvement may be due to the formation of protrusions or sharp edges that could act as emission sites.

Even under ultrahigh vacuum conditions sputtering or desorption of material from the anode can be caused due to the high energy electrons emitted from the sample. This may result in deposition of material on the sample or in a destructive discharge. Positive ions will be accelerated towards the surface of the sample and may damage the surface, even if no plasma discharge occurs. One way to avoid these damaging effects is the use of lower voltages. This implies that smaller distances need to be employed to facilitate the field emission. At smaller distances, effects due to the surface roughness of the sample or the anode become more significant.

Simultaneous field emission and photoemission measurements from a (111) 1x1:H p-type natural diamond surface were reported by Bandis and Pate.[53] From these experiments it was found that the field emitted electrons originated from the valance band maximum. Fig. 13 shows the electron energy distribution for the simultaneous field emission and photoemission measurements.[53] In contrast the photoemission process

involved emission from the conduction band. For boron doped polycrystalline diamond films Glesener and Morrish found no dependence of the field emission on temperature, and they also suggest that the electrons originate from the valence band.[54] To date there have been no studies that confirmed field electron emission originating from the conduction band of diamond. Most studies on emission from diamond may be explained as electron emission from the valence band or from defect states. Only UV photoemission spectroscopy measurements, where UV radiation is employed to excite electrons from the valence band into the conduction band, have studied the electron emission from the conduction band.

Supplying electrons to the conduction band remains a significant problem. Ideally a shallow n-type dopant could solve this issue. Then a field emission structure could consist of a highly n-type doped region at the electron injecting contact and lower doping in the bulk of the material. Nitrogen is a substitutional dopant and has been reported in concentrations of 10^{19} cm^{-3} in diamond.[55] It has been reported that high concentration of incorporated nitrogen could enhance electron emission.[27,29] According to theoretical [56] and experimental [57,58] studies the "shallowest" level of nitrogen is located about 1.5-2.1 eV below the conduction band minimum. Extremely high nitrogen concentrations would be necessary to get a n-type doping effect and to facilitate the electron injection at the back contact. There has been great difficulty in incorporating such large amounts of nitrogen into diamond. Alternatively, roughening of the interface at the contact may help circumvent this difficulty and lower the effective barrier for electron injection due to field enhancement at the rough interface.[27] A novel approach for CVD diamond deposition has been reported to enable the incorporation of large amounts of nitrogen into diamond.

Phosphorus is another substitutional impurity that may be a potential n-type dopant in diamond. For substitutional phosphorus an activation energy of 0.20 eV has been calculated.[56] Also the value for the equilibrium solubility of phosphorus in diamond is

expected to be low.[56] A doping effect due to a shallow level of phosphorus has also been found experimentally.[59] N-type conductivity and a corresponding value of 0.20-0.21 eV for the activation energy was measured for phosphorus implanted into high purity type IIa natural diamond.[60] Deeper levels with activation energies of 0.84-1.16 eV have been calculated [61,62] and measured experimentally.[63,64]

Lithium is an interstitial impurity in diamond and may be another potential n-type dopant. A donor level of 0.1 eV below the conduction band minimum has been reported.[56] But diffusion of lithium would result in an undesirable deterioration of the doping characteristics over time.[56] Also the solubility of lithium in diamond is predicted to be low.

The commonly observed non-uniformity in the emission from diamond surfaces [27] may also be a significant obstacle for the potential use of diamond in emission devices. This implies that the emission site density becomes a crucial characteristic to determine whether an emitting surface is suitable for practical applications. It has been estimated that an emission site density of the order of at least 10^6 to 10^7 sites/cm^2 is necessary for applications as field emission displays.[65] Figures 14 a) and b) show emission images of a carbon layer for 6.5 V/μm and 10 V/μm.[65] An image of a differently prepared carbon film for 10V/μm is shown in Figure 14 c).[65] A comparison of the emission site density for these two carbon films can be seen in Figure 15.[65] A reported increase in emission site density of CVD diamond films has been attributed to a pre-growth treatment.[66] Figure 16 shows the emission site density of a treated and an untreated area.[66].

However, uniform emission from diamond films has been reported in one study using a novel surface electron microscope that was operated in the field emission mode.[67,68] The instrumental limit for the field was 2V/μm. Since typical threshold fields in other reports are about an order of magnitude higher it may be conceivable that there is a uniform emission at low fields which becomes non-uniform at higher fields. This issue will need to

be resolved for most applications.

15.5 Conclusions

It is now evident that obtaining a true NEA is possible for diamond. Results indicate that a positive electron affinity is obtained for both adsorbate free and oxygen terminated surfaces. However, a NEA is obtained for hydrogen termination of all low index surfaces. It is interesting to note that more than a decade transpired between the first NEA measurements on (111) surfaces, and the discovery of a NEA for H-terminated (100) surfaces. It may be that the more tenacious bonding of oxygen to the (100) surface was at least partially responsible for the delayed observation.

The properties of thin metal layers on diamond have also indicated that these may be suitable for obtaining a NEA surface. The model used to describe this effect is based on two interfaces - the vacuum-metal interface and the metal-diamond interface. Within this model, to lower the effective electron affinity of this structure it is necessary that the metal-diamond interface changes the surface dipole of the diamond. A particularly encouraging result was found for Zr deposited on clean diamond surfaces and surfaces with oxygen or H adsorbates. Here it appears that the Zr displaces the oxygen or hydrogen termination.

The field emission is the most complicated and potentially least understood measurement. The combined photo and field emission measurements indicate that field emission from p-type diamond originates from electrons in the valence band. Similarly, many studies have indicated lower field emission thresholds for diamond with significant defect density. This again suggests that the emission does not involve electrons in the conduction band. While conduction band emission has been suggested for nitrogen doped diamond, the role of defects needs to be further explored.

The two most pressing questions in the field emission studies is verifying if field

emission from the conduction band has been obtained and understanding the non-uniform emission. Certainly the development of a process to obtain shallow n-type doping would go a long way to solving each of these problems.

Even without the development of an n-type dopant it seems likely that diamond with defects may substantially improve the emission character of various pointed and flat surfaces. Preparation of actual device structures may be necessary to determine if the current status is sufficient for the applications.

Diamond has been the wide gap semiconductor that has been most often considered for emission applications, but recent studies have indicated a negative electron affinity for both BN and AlN. It appears that n-type doping of these materials is also problematic, but other approaches may be available for supplying electrons to the conduction band.

This review has neglected some aspects of field emission. The most notable of these may be the beneficial effects of roughness and interfaces. However, the complexities of the processes may provide a real challenge for future research.

References

1. Himpsel, F.J., J.A. Knapp, J.A. van Vechten, D.E. Eastman, Phys.Rev. B20 (1979), 624.
2. Pate, B.B. (1986). Surf. Sci. **165**, 83.
3. R. Gomer, *Field Emission and Field Ionization*, (Harvard Press, Cambridge, 1961).
4. Zangwill, A (1988), *Physics at Surface*, (Cambridge).
5. R. J. Nemanich, P. K. Baumann, M. C. Benjamin, S. W. King, J. van der Weide, R. F. Davis, "Negative electron affinity surfaces of aluminum nitride and diamond" Diamond Related Mat. 5 (1996) 790-796
6. J. van der Weide, R. J. Nemanich, "Argon and Hydrogen Plasma Interactions on Diamond (111) Surfaces; Electronic States and Structure", Appl. Phys. Lett. 62 (1993), 1878-1880.
7. C. Bandis and B.B. Pate, "Electron Emission Due to Exciton Breakup from Negative Electron Affinity Diamond," Phys. Rev. Lett. 74 (1995), 777.
8. P. K. Baumann, R. J. Nemanich, "Surface Cleaning, Electronic States and Electron Affinity of Diamond (100), (111) and (110) Surfaces" submitted to J. Appl. Phys.
9. G.T. Mearini, I.L. Krainsky, J.A. Dayton, Jr., Y. Wang, C.A. Zorman, J.C. Angus, D.F. Anderson, "Stable secondary electron emission from chemical vapor deposited diamond films coated with alkali-halides," Appl. Phys. Lett. 66 (1995), 242-244.
10. D.P. Malta, J.B. Posthill, T.P. Humphreys, R.E. Thomas, G.G. Fountain, R.A. Rudder, G.C. Hudson, M.J. Mantini, and R.J. Markunas, "Secondary electron emission enhancement and defect contrast from diamond following exposure to atomic hydrogen," Appl. Phys. Lett. 64 (1994), 1929-1931.
11. R.E. Thomas, T.P. Humphreys, C. Pettenkofer, D.P. Malta, J.B. Posthill, M.J. Mantini, R.A. Rudder, G.C. Hudson R.J. Markunas, "Influence of surface

terminating species on electron emission from diamond surfaces," Mat. Res. Soc. Symp. Proc. vol 416 (1996), 263-274.

12. R. J. Nemanich, L. Bergman, K. F. Turner, J. van der Weide and T. P. Humphreys, "Properties of Interfaces of Diamond," Trieste Semiconductor Symposium on Wide-Band-Gap Semiconductors, Physica B 185 (1993), 528-538.
13. van der Weide, J., Z. Zhang, P. K. Baumann, M. G. Wensell, J. Bernholc and R. J. Nemanich, "Negative Electron Affinity Effects on the Diamond (100) Surface", Physical Review B 50 (1994), 5803-5806.
14. van der Weide, J., and R. J. Nemanich,"Angle-Resolved Photoemission of Diamond (111) and (100) Surfaces; Negative Electron Affinity and Band Structure Measurements", J. Vac. Sci. Technol. B 12, 2475-2479 (1994).
15. P. K. Baumann and R. J. Nemanich, "Negative Electron Affinity Effects on H Plasma Exposed Diamond (100) Surfaces", Diamond Relat. Mat. 4 (1995), 802-805.
16. P.K. Baumann, T.P. Humphreys and R.J. Nemanich, "Comparison of Surface Cleaning Processes for Diamond (100)," Mat. Res. Soc Symp. Proc. vol 339 (1994), 69-74.
17. M.J. Rutter and J. Robertson, submitted to Phys. Rev. B
18. M.W. Geis, J.C. Twichell, J. Macaulay, and K. Okano, "Electron field emission from diamond and other carbon materials after H2, O2, and Cs treatment," Appl. Phys. Lett. 67 (1995), 1328-1330.
19. O. M. Küttel, O. Gröning, E. Schaller, L. Diederich, P. Gröning and L Schlapbach, "Electron field emission from a caesiated NEA diamond (100) surface: an activation concept" Diamond Related Mat. 5 (1996) 807-811.
20. J. van der Weide, and R. J. Nemanich, "Schottky Barrier Height and Negative Electron Affinity of Titanium on (111) Diamond," J. Vac. Sci. Technol. B 10 (1992), 1940-1943 .

21. J. van der Weide, and R. J. Nemanich,"Influence of Interfacial Hydrogen and Oxygen on the Schottky Barrier of Nickel on (111) and (100) Diamond Surfaces", Physical Review B49 (1994), 13629-13637.

22. P.K. Baumann, R.J. Nemanich, "Characterization of Co-diamond (100) interfaces: electron affinity and Schottky barrier," Appl. Surf. Sci.104/105 (1996) 267; "Negative electron affinity effects and Schottky barrier height measurements od metals on diamond (100) surfaces," Mat. Res. Soc. Symp. Proc. vol. 416 (1996), 157-162. and "Electron Affinity and Schottky Barrier Height of Metal - Diamond Interfaces": J. Vac. Sci. Tech. B 15(4) (1997) in press

23. P. K. Baumann, R. J. Nemanich, "Characterization of Copper - Diamond (100), (111) and (110) Interfaces: Electron Affinity and Schottky Barrier" submitted to Phys. Rev. B

24. P.K. Baumann and R.J. Nemanich, "Electron Affinity and Schottky Barrier Height of Metal Diamond (100), (111) and (110) Interfaces" submitted to J. Appl. Phys.

25. P. K. Baumann, T. P. Humphreys, R. J. Nemanich, K. Ishibashi, N. R. Parikh, L. M. Porter and R. F. Davis, "Epitaxial Cu Contacts on Semiconducting Diamond", Diamond Related Mat. 3 (1994), 883-886.

26. Bandis, C., D. Haggery, and B.B. Pate, "Electron emission properties of the NEA (111) 2x1 diamond -TiO interface," Mat. Res. Soc. Symp. Proc. vol. 339 (1994), 75-81.

27. M.W. Geis, J.C. Twichell, N.N. Efremow, K. Krohn, and T.M. Lyszczarz, "Comparison of electric field emission from nitrogen-doped, type Ib diamond, and boron doped diamond," Appl. Phys. Lett. 68 (1996), 2294-2296.

28. W. Zhu, G.P. Kochanski, S. Jin, L. Seibles, D.C. Jacobson, M. McCormack and A.E. White, Appl. Phys. Lett. 67 (1995), 1157-1159.

29. K. Okano, S. Koizumi, S.R.P. Silva, G.A.J. Amaratunga, "Low-threshold cold

cathodes made of nitrogen-doped chemical-vapour-deposited diamond," Nature 381 (1996), 140-141.

30. P.V. Latham, High Voltage Vacuum Insulation, edited by R.V.Latham, Academic Press, San Diego (1995).
31. Z. Feng, I. G. Brown and J. W. Ager III, "Electron emission from chemical vapor deposited diamond and amorphous carbon films observed with a simple field emission device" J. Mater. Res. vol. 10 (1995) 1585-1588.
32. A. A. Talin, L. S. Pan, K. F. McCarthy, T. E. Felter, H. J. Doerr and R. F. Bushah, "The relationship between the spatially resolved field emission characteristics and the raman spectra of a nanocrystalline diamond cold cathode" Appl. Phys. Lett. vol. 69 (1996) 3842-3844.
33. C. Wang, A. Garcia, D.C. Ingram, M. Lake, and M.E. Kordesch, Electron. Lett. 27 (1991), 1459.
34. N.S. Xu, R.V. Latham and Y. Tzeng, Electron. Lett. 29 (1993), 1596.
35. W. Zhu, G.P. Kochanski, S. Jin, "Electron field emission properties of diamond" Mat. Res. Soc. Symp. Proc. vol. 416 (1996) 443-448.
36. Z.-H. Huang, P.H. Cutler, N.M. Miskovsky and T.E. Sullivan, Appl. Phys. Lett. 65 (1994), 2562-2565.
37. N.M. Miskovsky, P.H. Cutler and Z.-H. Huang, J. Vac. Sci. Technol. B 14 (1996) 2037 - 2040.
38. J. Prins, "Ion-implantation and diamond - some recent results on growth and doping", Thin Solid Films vol. 212 (1992) 11-18.
39. J. Prins, "Ion-implanted structures and doped layers in diamond". Materials Science Reports vol. 7 (1992) 271-364.
40. M. Geis, N. Efremow, J. Woodhouse, M. Mcalese, M. Marchywka, D. Socker and J. Hochedez, "Diamond cold cathode", IEEE Elect. Dev. Lett. vol. 12 (1991) 456-

459.

41. N. S. Xu, Y. Tzeng and R. V. Latham, J. Phys. D: Appl Phys., 26 (1993) 1776
42. J. Liu, V. V. Zhirnov, A. F. Myers, G. J. Wojak, W. B. Choi, J. J. Hren, S. D. Wolter, M. T. McClure, B. R. Stoner and J. T. Glass, J. Vac. Sci Technol. B 13 (1995) 422.
43. W. B. Choi, J. J. Cuomo, V. V. Zhirnov, A. F. Myers and J.J. Hren, Appl. Phys. Lett. 68 (1996) 720.
44. W. B. Choi, J. Liu, M. T. McClure, A. F. Myers, V. V. Zhirnov, J. J. Cuomo and J.J. Hren, J. Vac. Sci. Technol. B 14 (1996) 2050.
45. V. Raiko, R. Spitzl, B. Aschermann, D. Theirich, J. Engemann, N. Puteter, T. Habermann, G. Müller, Thin Solid Films 290-291 (1996) 190.
46. E. I. Givargizov, V. V. Zhirnov, A. N. Stepanova, E. V. Rakova, A. N. Kieselev, P. S. Plekhanov, "Microstructucture and field emission of diamond particles on silicon tips" Appl. Surf. Sci. vol. 87/88 (1995) 24-30.
47. V. V. Zhirnov "On the cold emission mechanism of diamond coated tips" J. de Physique IV vol. 6 (1996) C5-107 - C5-112.
48. D. M. Gruen, X. Pan, A. R. Krauss, S. Liu, J. Luo, C. M. Foster "Deposition and characterization of nanocrystalline diamond films" J. Vac. Sci. Technol. A vol. 12 (1994) 1491-1495.
49. D. M. Gruen, C. D. Zuiker, A. R. Krauss, "Diamond films grown from fullerene precursors" Proc. of the SPIE - The International Society for Optical Engineering vol. 2530 (1995) 2-13.
50. C. D. Zuiker, A. R. Krauss, D. M. Gruen, X. Pan, J. C. Li, R. Csencsits, A. Erdemir, C. Bindal, G. Fenske, "Physical and tribological properties of diamond films grown in argon-carbon plasmas" Thin Solid Films vol. 270 (1995) 154-159.
51. A. R. Krauss, personal communication

52. O. Gröning, O. M. Küttel, E. Schaller, P. Gröning and L Schlapbach, "Vacuum arc discharges preceding high electron field emission from carbon films" Appl. Phys. Lett. vol. 69 (1996) 476-478.

53. C. Bandis, B.B. Pate, Appl. Phys. Lett. 69 (1996) 366.

54. J. W. Glesener and A. A. Morrish, Appl. Phys. Lett. 69 (1996) 785.

55. T. Evans, The properties of natural and synthetic diamond, edited by J.E. Field, Academic Press, London (1992) 259

56. S.A. Kajihara, A. Antonelli, J. Bernholc and R. Carr Phys. Rev. Lett. vol. 66 (1991) 2010.

57. W.J.P. Enkevort and E.H. van Versteegen, J. Phys.: Condens. Matter vol. 4 (1992) 2361.

58. R.G. Farrer, Solid State Commun., vol. 7 (1969) 685

59. K. Okano, H. Kiyota, T. Iwasaki, T. Kurosu, M. Iida and T. Nakamura, New Diamond Science and Technology, MRS Int. Conf. Proc. (1991) 917

60. J.F. Prins, Diamond Relat. Mat. vol. 4 (1995) 580

61. K. Jackson, M.R. Pederson and J.G. Harrison, Phys. Rev. B, vol. 41 (1990) 12641

62. V.V. Tokiy, N.D. Samsonenko, D.L. Savina and S.V. Gorban, Proc of the 2nd Int. Conf. on the Applications of Diamond Films and Related Materials, August 25-27, 1993, Japan, MYO, Tokyo p.757

63. M.I. Landstrass, M.A. Plano, D. Moyer, S.P. Smith, and R.G. Wilson, Diamond Materials, Electrochemical Society (1991) 574.

64. M. Kamo, H. Yarimoto, T. Ando and Y. Sato, New Diamond Science and Technology, MRS Int. Conf. Proc. (1991) 637.

65. A. A. Talin, B. F. Coll, E. P. Menu, J. Markhalm and J. E. Jaskie, "Carbon cathode requirements and emission characterization for low-voltage field emission displays", Proc. of the 1st Specialist Meeting on Amorphous Carbon, Cambridge, UK, July 31,

1997.

66. Z. L. Tolt, R. L. Fink and Z. Yaniv, "Electron emission from patterned diamond flat cathodes", Proc. of IVMC'97, J. Vac. Sci. Technol. A

67. J.D. Shovlin and M.E. Kordesch, "Electron emission from CVD diamond and dielectric breakdown," Appl. Phys. Lett. 65 (1994), 863-865.

68. J.D. Shovlin, M.E. Kordesch, D. Dunham, B.P. Tonner, W. Engel, "Synchrotron radiation photoelectron emission microscopy of CVD diamond electron emitters", J. Vac. Sci. Technol. A13 (1995), 1111-1115.

Table 1. The UPS spectral width for different diamond (100) and (110) surface terminations. The electron affinity or presence of a NEA is deduced using Eq. 1.

Surface	UPS Spectral Width (eV)	Electron Affinity (eV)
C(100):H	15.7	NEA
C(100) (clean)	15.05	0.65
C(100):O	14.2	1.50
C(110):H	15.7	NEA
C(110) (clean)	15.1	0.60
C(110):O	14.3	1.40

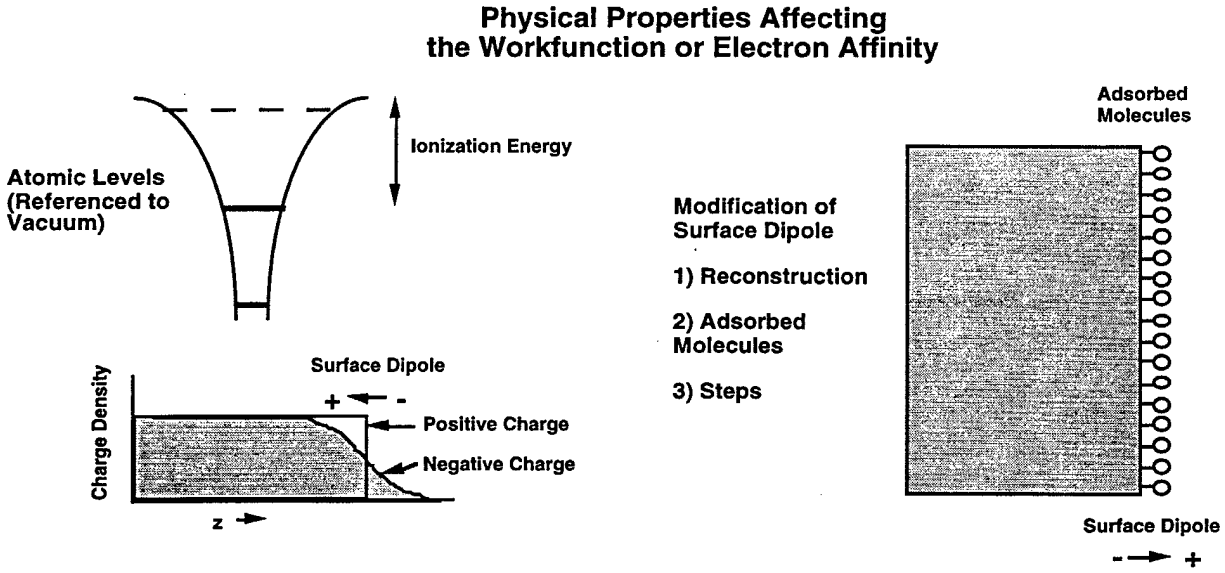

Fig. 1 A representation of the effects which contribute to the work function (or electron affinity) of any material. While the atomic levels are an intrinsic property of the material, changes in the surface bonding can substantially affect the work function or electron affinity.

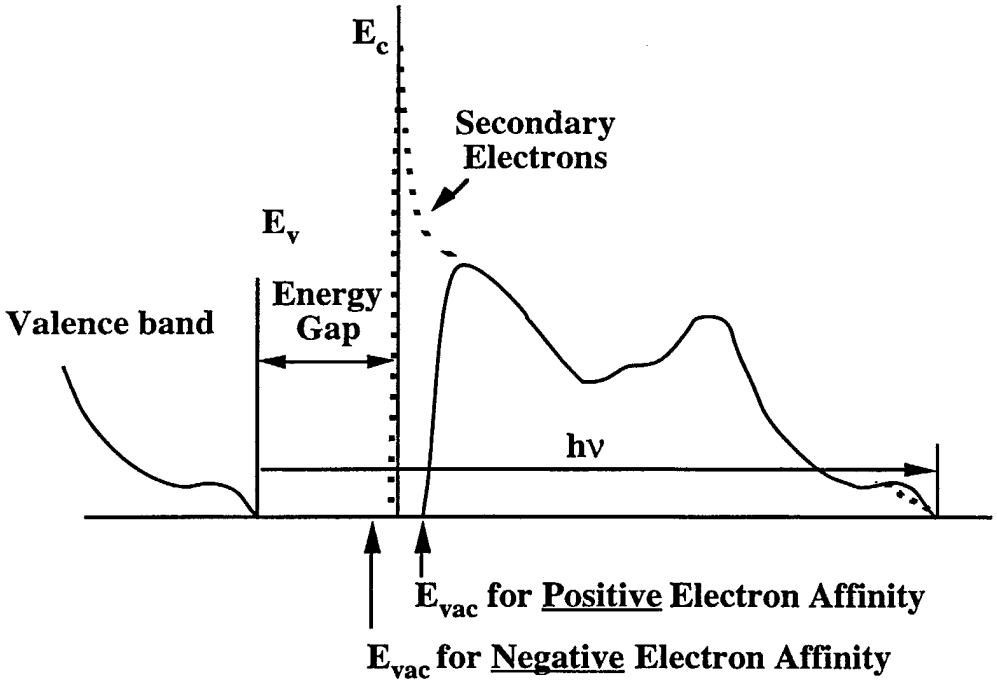

Fig. 2 A schematic of how NEA affects the photoemission spectra. For a NEA surface the spectra is broadened to lower kinetic energy and a peak due to quasi thermalized electrons is detected also at the lowest kinetic energy. [6]

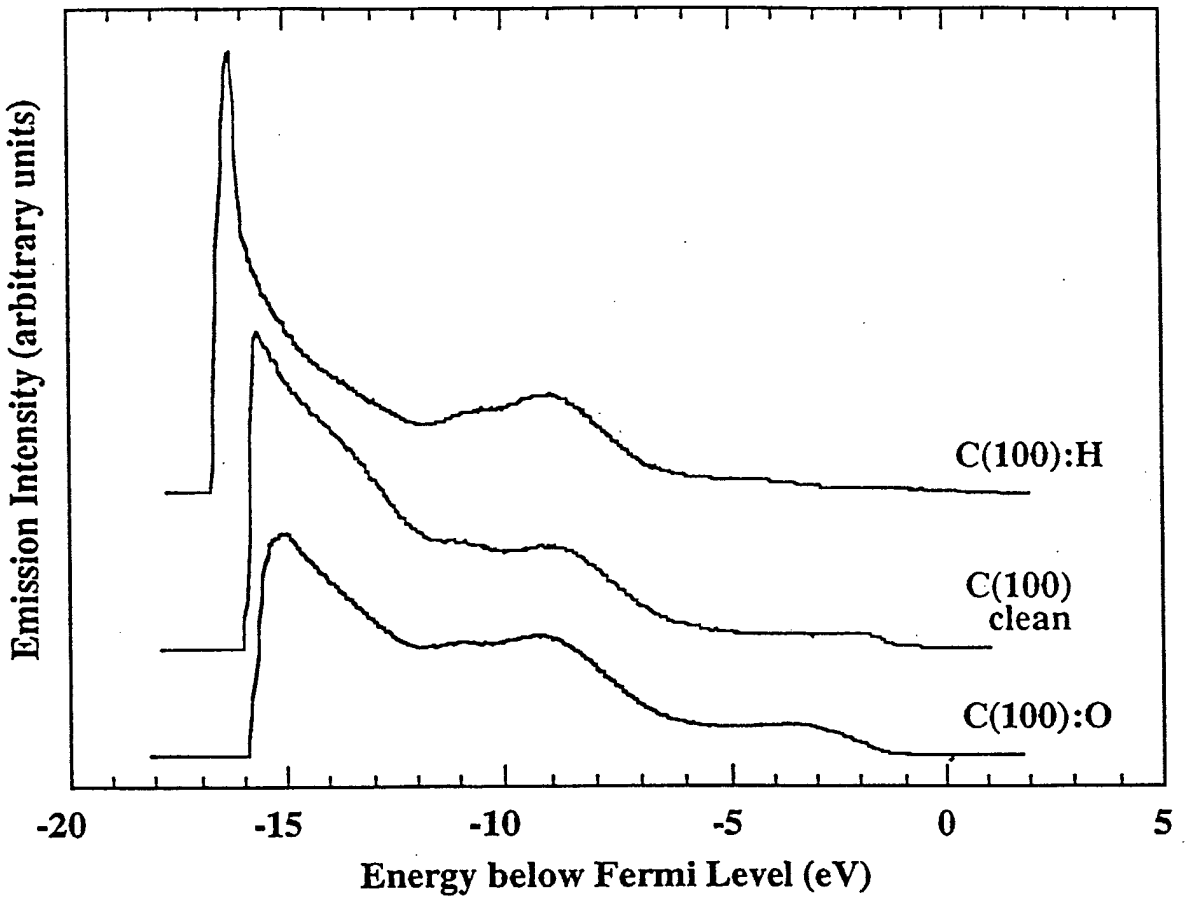

Fig. 3 Photoemission spectra of oxygen, hydroterminated and clean diamond (100) surfaces. The broadening of the spectral width and the sharp feature at high (negative) binding energy (i.e. low kinetic energy) are indicative of a NEA.

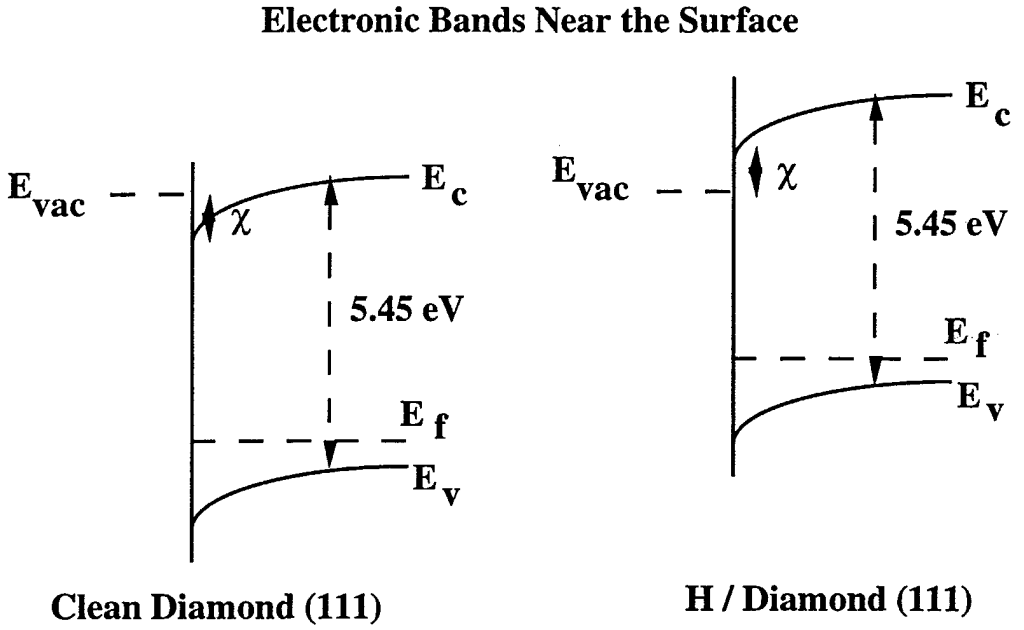

Fig. 4 The band alignments of clean diamond and H terminated diamond surfaces. Note that the figures have been aligned at the vacuum level.

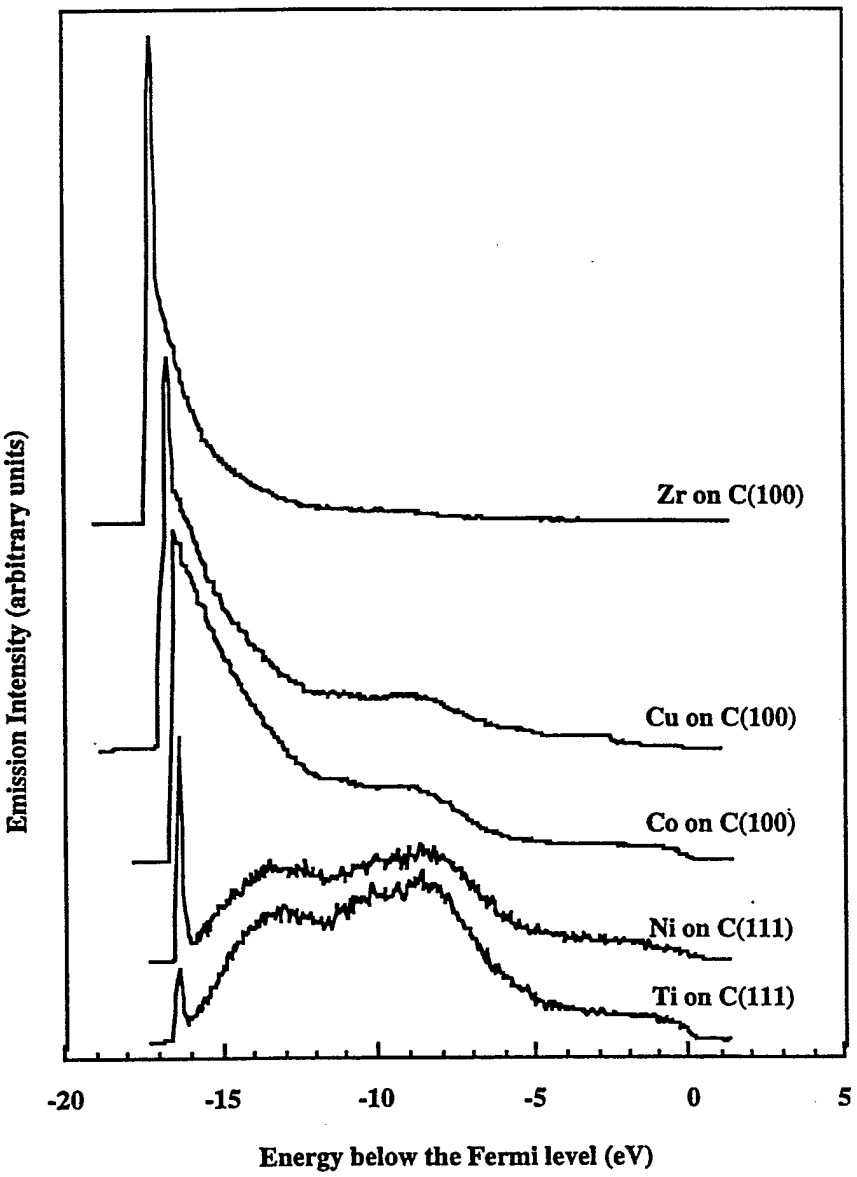

Fig. 5. UV-photoemission spectra of diamond surfaces with thin metal overlayers. The metal thicknesses correspond to several monolayers.

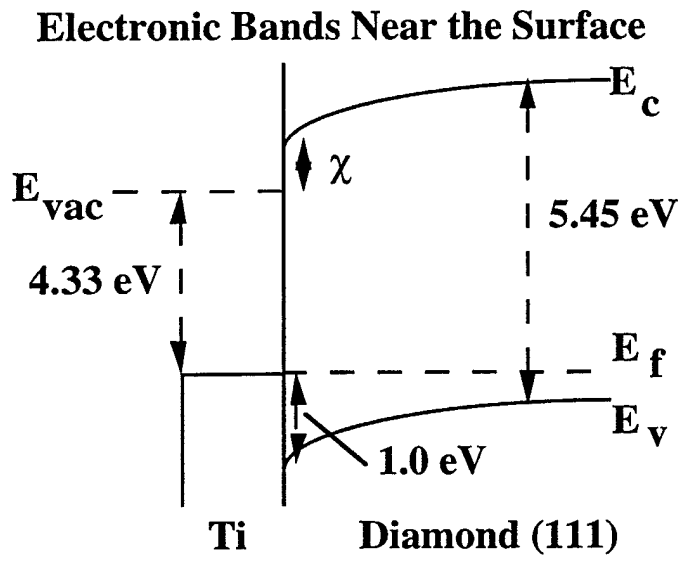

The electron affinity is then given by

$$\chi = (\psi_m + \varphi_p) - E_g$$

$$= (4.33 + 1.0) - 5.45$$

$$= -0.1 \text{ eV}$$

Fig. 6. The band structure at the surface of diamond with a thin metal coverage. The electron affinity can be deduced from the Schottky barrier, the metal work function and the diamond bandgap. The numbers for Ti on diamond (111) are illustrated.

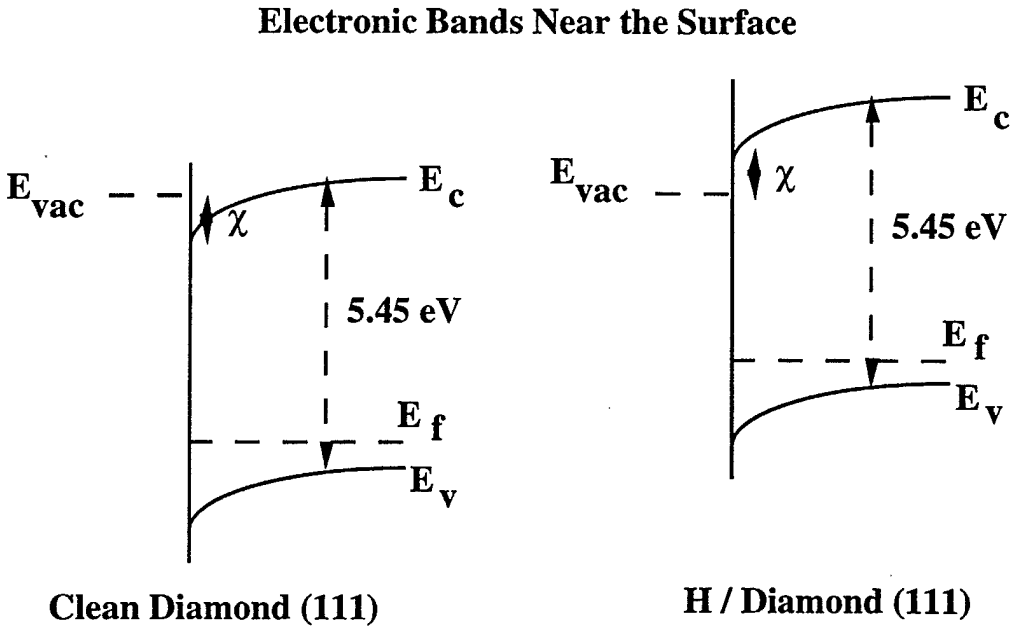

Fig. 7 Schematic band diagram of Ti on clean and H-terminated diamond surfaces. Note that the figures have benn aligned at the vacuum level.

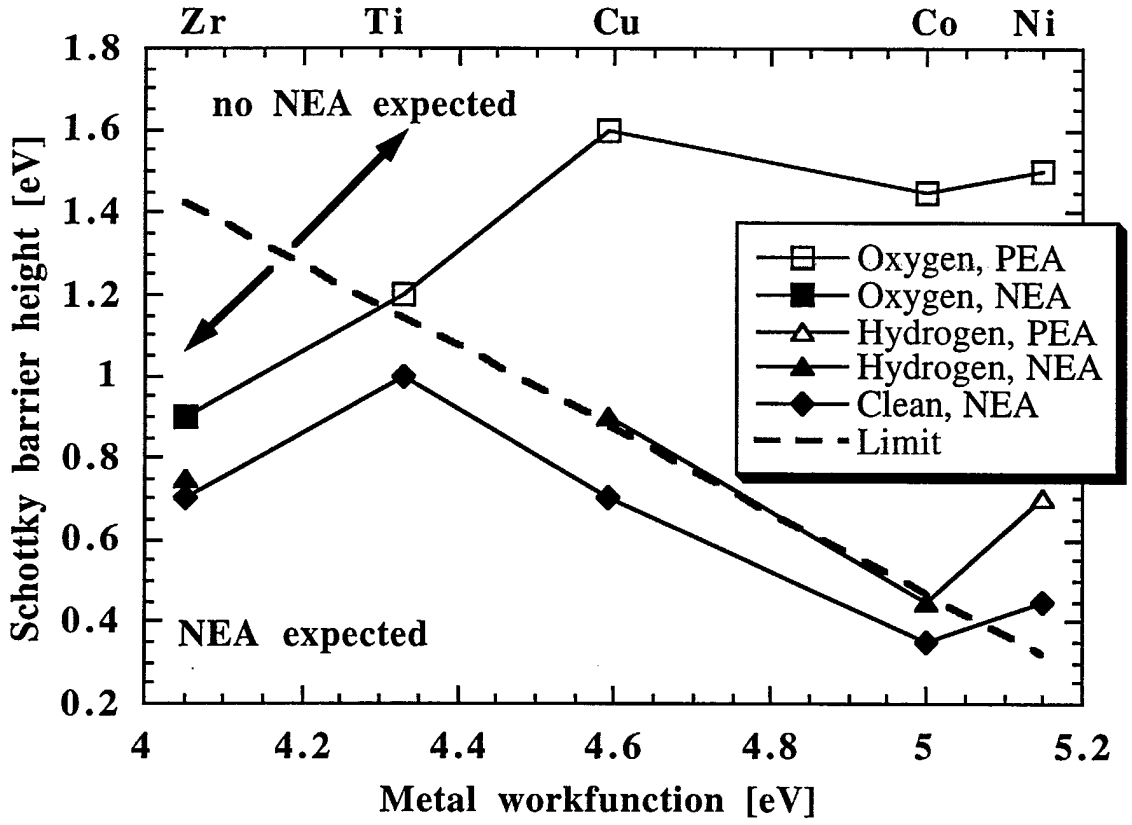

Fig. 8. Diagram of the Schottky barrier height vs. metal workfunction for Ti, Zr, Cu, Co and Ni. The dashed line represents the limit for which a NEA is expected for metal - diamond interfaces according to equation (2). Thus a NEA is expected for data points below this dashed line and a positive electron affinity for those above. The experimental data for Ti, Zr, Cu, Co and Ni are plotted. The filled markers correspond to an experimentally observed NEA and the empty markers indicate an experimentally observed positive electron affinity.[24]

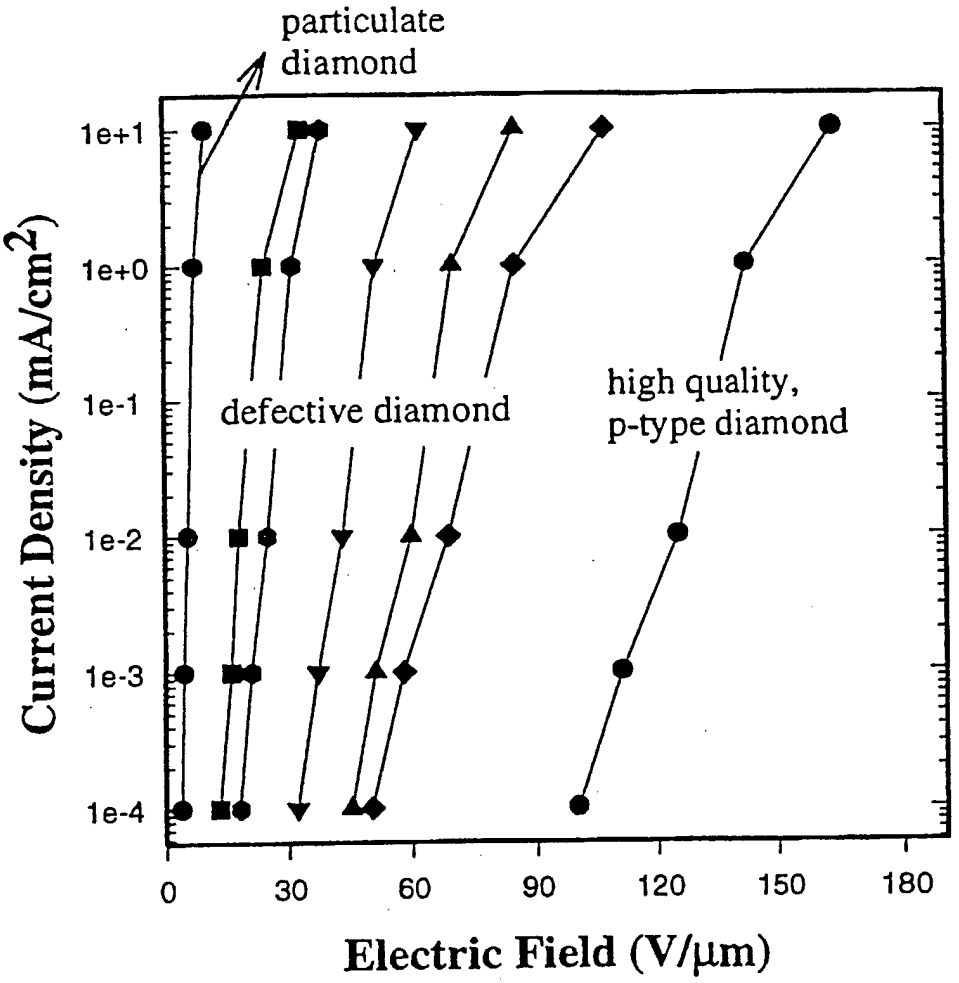

Fig. 9 Plot of the emission current densities vs. field required for emission from p-type CVD diamond, defective undoped diamond and nanometer size diamond powder.[33]

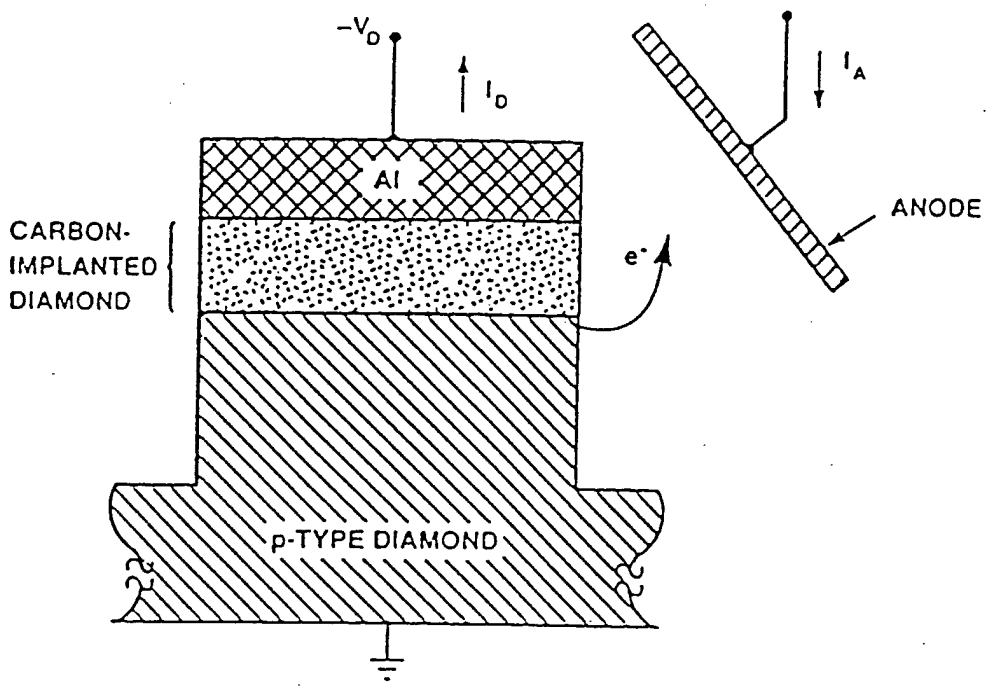

Fig. 10 Schematic of the cold cathode based on an all diamond p-n junction.[38]

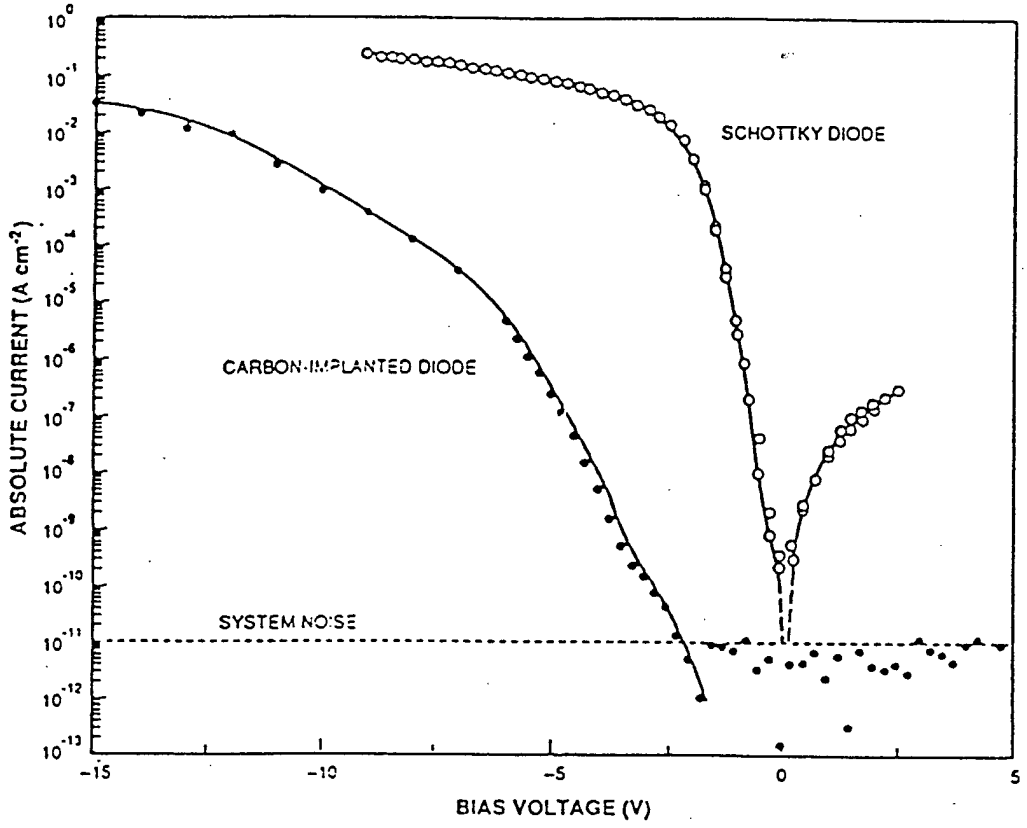

Fig. 11 Diode current vs. applied voltage for the carbon ion implanted diode was compared to that of an aluminum Schottky contact on p-type diamond. Illustrates the measured I-V characteristics for both structures.[38]

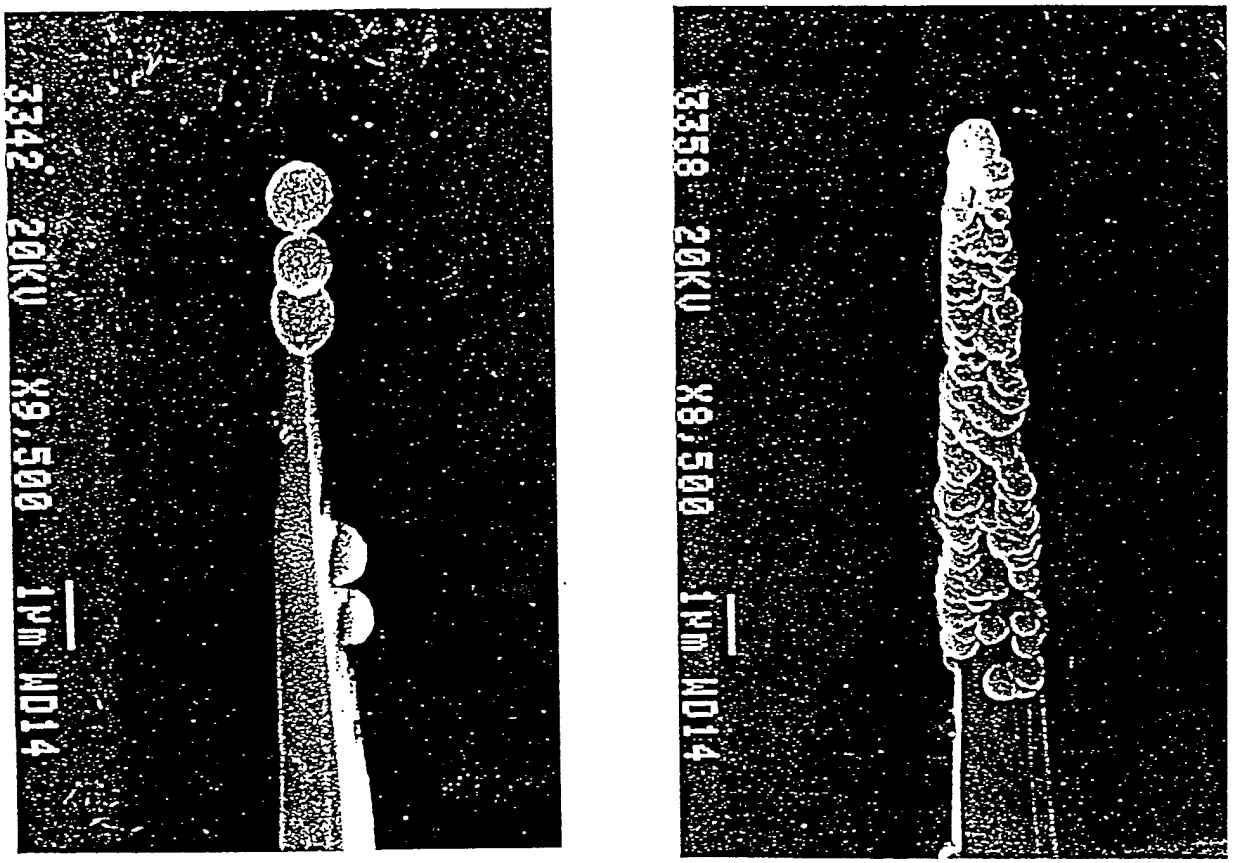

Fig. 12. Distinct diamond particles on the silicon tips. a) single-particle-type diamond coverage. b) Conglomerate of diamond particles.[45]

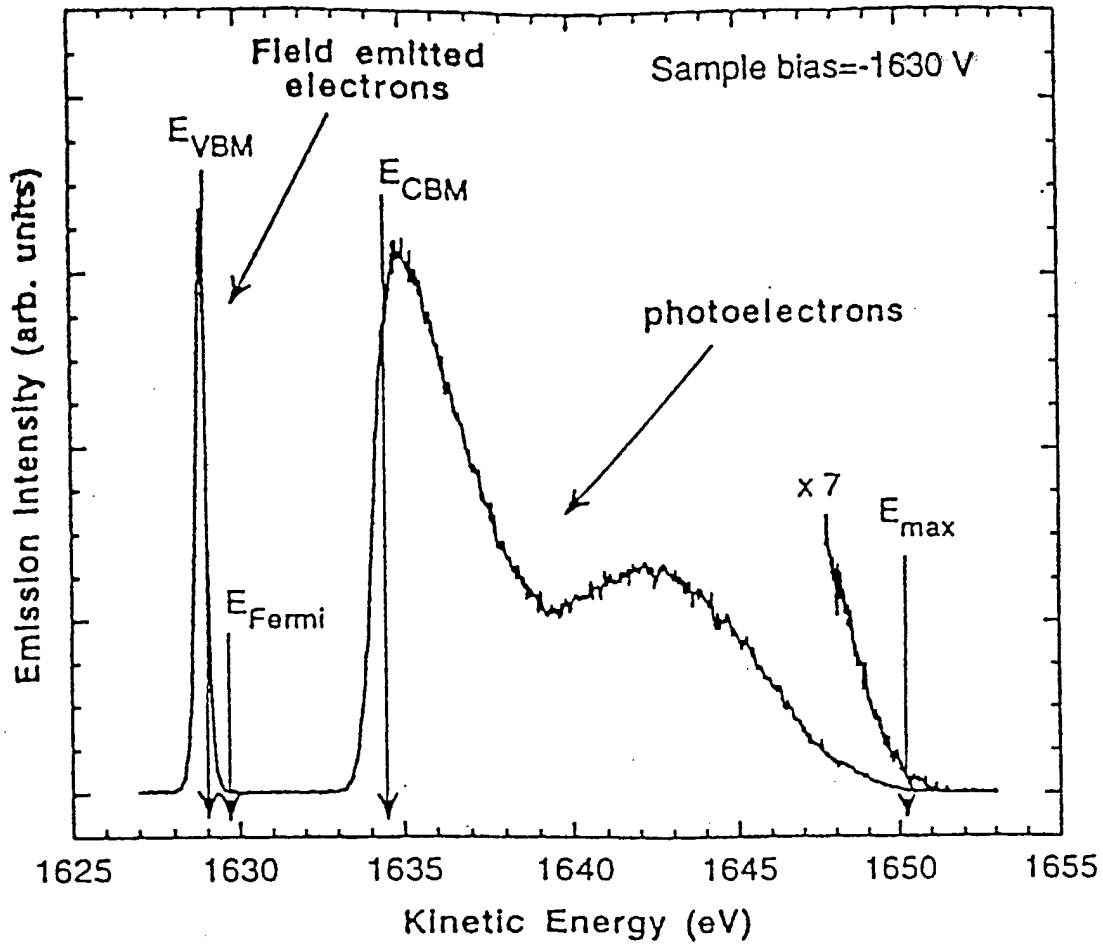

Fig. 13 Electron energy distribution for the simultaneous field emission and photoemission measurements on C(111)1x1:H. The energy position of the field emitted electrons corresponds to the valence band maximum.[51]

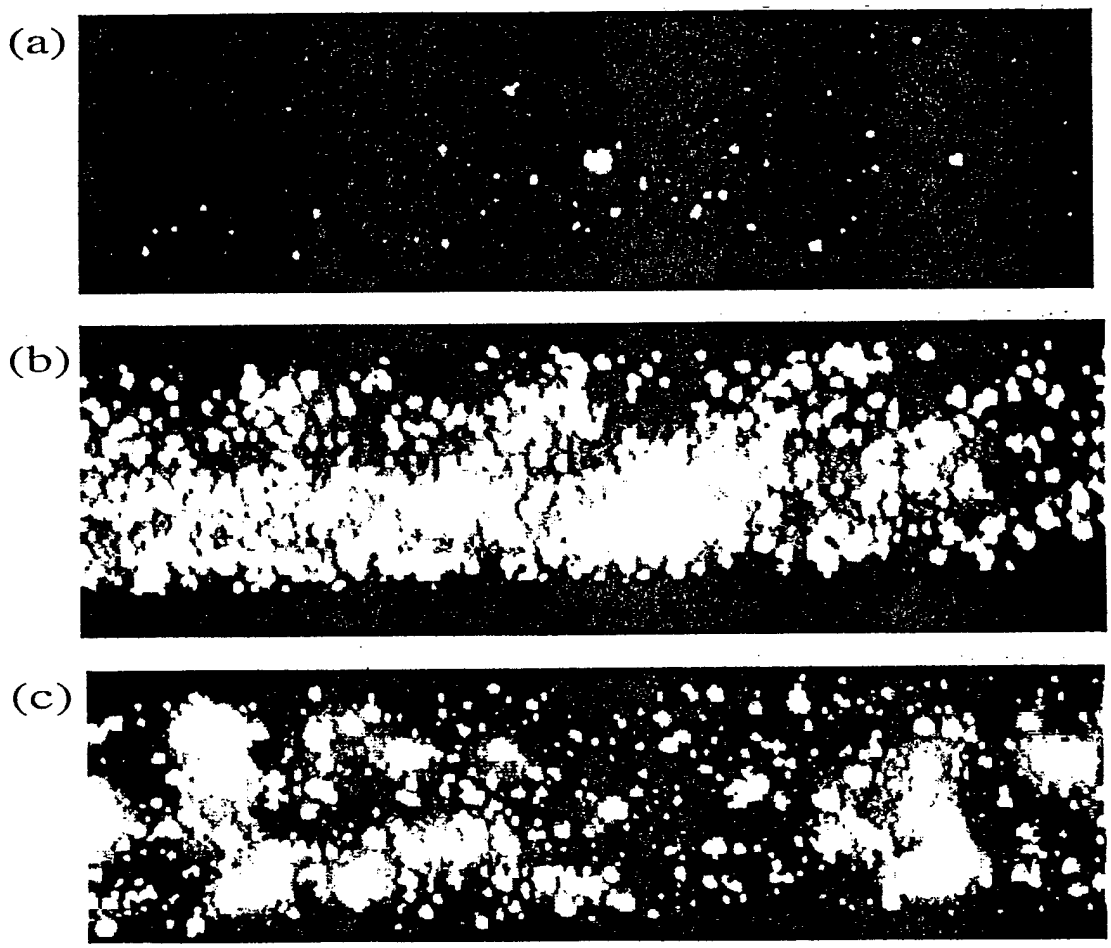

Fig. 14 Field electron emission from a) cathode 1, 6.5 V/μm, b) cathode 1, 10 V/μm, c) cathode 2, 10V/μm.[65]

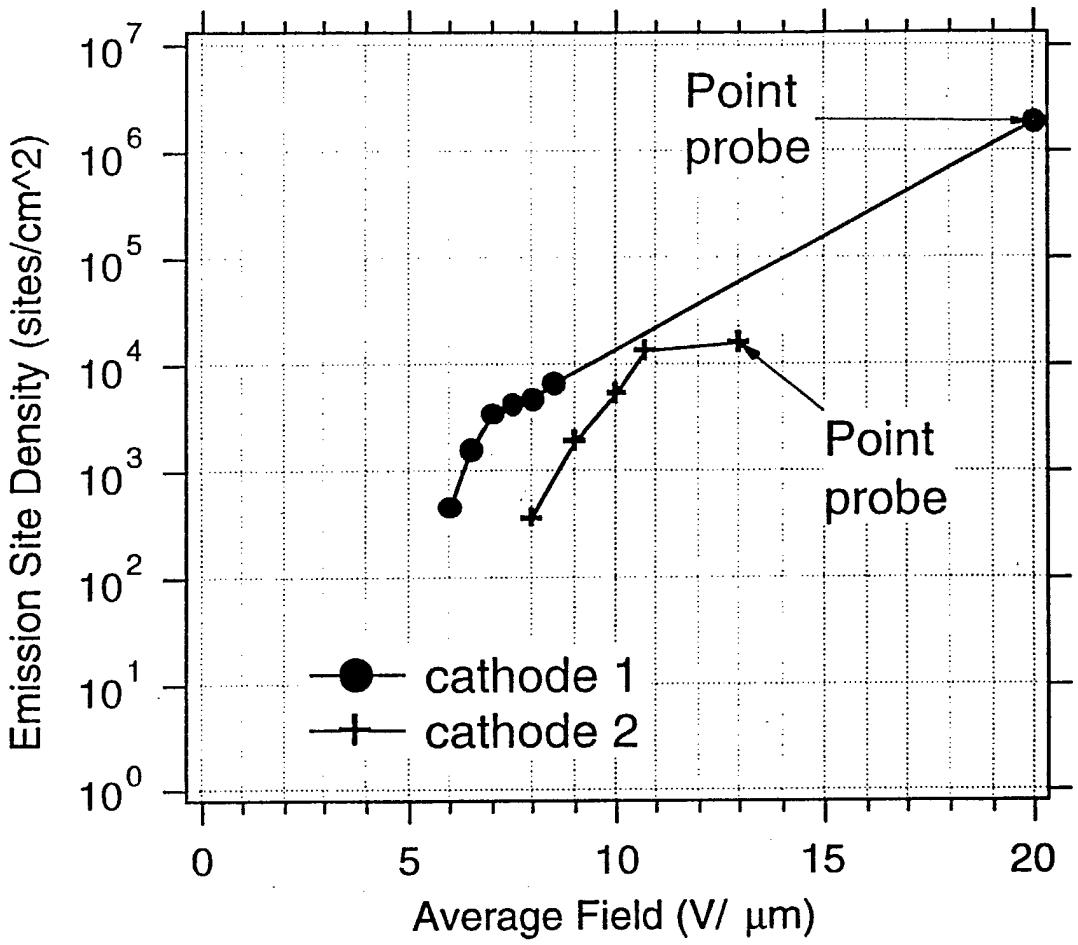

Fig. 15 Plot of the emission site density versus average field for cathodes 1 and 2.[65]

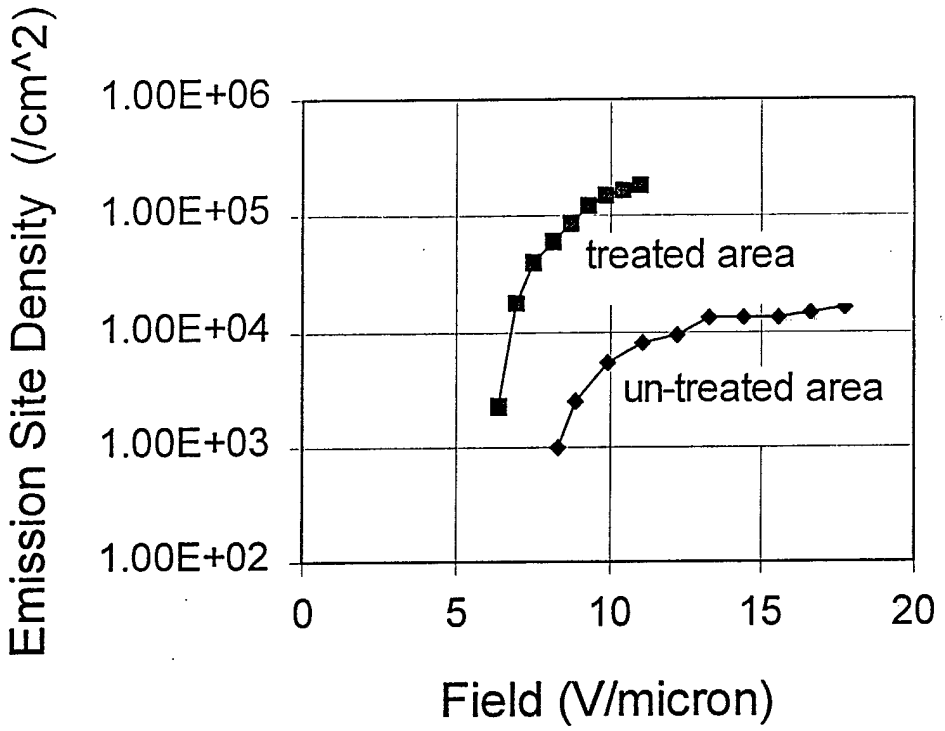

Fig. 16 Plot of the emission site density versus field for treated and untreated areas of the substrate.[66]

V. Distribution List

Dr. Colin Wood Office of Naval Research Electronics Division, Code: 312 Ballston Tower One 800 N. Quincy Street Arlington, VA 22217-5660	3
Administrative Contracting Officer Office of Naval Research Atlanta Regional Office 100 Alabama Street, Suite 4R15 Atlanta, GA 30303	1
Director, Naval Research Laboratory ATTN: Code 2627 Washington, DC 20375	1
Defense Technical Information Center 8725 John J. Kingman Road, Suite 0944 Ft. Belvoir, VA 22060-6218	2